Critical Reviews in Biochemistry and Molecular Biology, 36(5):435–499 (2001)

Lens Crystallins and Their Microbial Homologs: Structure, Stability, and Function

*** Dedicated to Prof. Ephrain Katchalski-Katzir on the occasion of his 85th birthday.**

Rainer Jaenicke[1,2] and Christine Slingsby[2]*

[1]Institut für Biophysik und Physikalische Biochemie, Universität Regensburg, D-93040 Regensburg, Germany; [2]Department of Crystallography, Birkbeck College, University of London, London WC1E 7HX, United Kingdom

Referee: Franz Schmid, Biochemicshes Laboratorium, Universitaet Bayeuth, D-95440 Bayeuth, Germany

ABBREVIATIONS USED

Amino acids are abbreviated using the single-letter code; αC (αA and αB): α-crystallin, (homologous αA and αB genes); βA1, βA2, βA3, βA4, βB1, βB2, βB3: different types of acidic and basic β-crystallins; $\beta B2\Delta_{NC}$ and $\beta B2\text{-}L_{\gamma B}$: βB2-crystallin, truncated at N- and C-terminal end and βB2-crystallin with its natural linker replaced by γB linker; γB, γB-N, γB-C, $\gamma B\text{-}C_{\Delta y174}$, and $\gamma B\text{-}L_{\beta B2}$: γB-crystallin, its isolated N- and C-terminal domains, isolated C-terminal domain of γB lacking its C-terminal tyrosin residue, and γB-crystallin with its natural linker replaced by βB2-linker, respectively; BγS and HγS: bovine and human γS-crystallin; γS-N, γS-C: isolated N- and C-terminal domains of γS-crystallin; CD: circular dichroism; CP: circular permutation or circularly permuted; $c_{1/2,urea}$, $c_{1/2,GdmCl}$: denaturant concentrations at midpoint of N→U transition; 3D: three-dimensional; ΔG, ΔΔG, and $\Delta G^{\ddagger}$: Gibbs free energy, difference of free energies and free energy of activation, respectively; GdmCl, GdmSCN: guanidinium chloride and thiocyanate, respectively; Hsp, sHsp: heat shock protein, small heat shock protein; Ig: immunoglobulin; IR: infrared; NMR: nuclear magnetic resonance; K, k : equilibrium constant and rate constant, respectively; N, U, I : native, unfolded and intermediate states; PS, PS-N, PS-C: protein S from *Myxococcus xanthus* and its N- and C-terminal domains, respectively; S1a, S1b, S2a, S3a: homologous spherulin proteins from *Physarum polycephalum*; SMPI: proteinase inhibitor from *Streptomyces nigrescens*; T_m, T_c : temperatures of thermal denaturation and phase separation, respectively: WmKT: yeast killer toxin from *Williopsis mrakii*.

* Corresponding author: Address: Ostpreussen Str. 12, D-65824 Schwalbach a.Ts. (Germany), Phone: +49-6196-807789. FAX: +49-6196-807790. E-mail: rjaenicke@gmx.de

ABSTRACT: abg-Crystallins are the major protein components in the vertebrate eye lens — a as a molecular chaperone and b and g as structural proteins. Surprisingly, the latter two share some structural characteristics with a number of microbial stress proteins. The common denominator is not only the Greek key topology of their

1040-9238/01/$.50

polypeptide chains but also their high intrinsic stability, which, in certain microbial crystallin homologs, is further enhanced by high-affinity Ca^{2+}-binding. Recent studies of natural and mutant vertebrate bg-crystallins as well as spherulin 3a from *Physarum polycephalum* and Protein S from *Myxococcus xanthus* allowed the correlation of structure and stability of crystallins to be elucidated in some detail. From the thermodynamic point of view, stability increments come from (1) local interactions involved in the close packing of the cooperative units, (2) the all-b secondary structure of the Greek-key motif, (3) intramolecular interactions between domains, (4) intermolecular domain interactions, including 3D domain swapping and (v) excluded volume effects due to "molecular crowding" at the high cellular protein concentrations. Apart from these contributions to the Gibbs free energy of stability, significant kinetic stabilization originates from the high activation energy barrier determining the rate of unfolding from the native to the unfolded state. From the functional point of view, the high stability is responsible for the long-term transparency of the eye lens, on the one hand, and the stress resistance of the microorganisms in their dormant state on the other. Local structural perturbations due to chemical modification, wrong protein interactions, or other irreversible processes may lead to protein aggregation. A leading cataract hypothesis is that only after a-crystallin, a member of the small heat-shock protein family, is titrated out does pathological opacity occur. Understanding the structural basis of protein stability in the healthy eye lens is the route to solve the enormous medical and economical problem of cataract.

KEY WORDS: cataract, crystallins, eye lens, domain interactions, protein stability, stress proteins.

I. INTRODUCTION

Recent high-resolution X-ray and NMR analyses of a number of microbial stress proteins such as spherulin (S3a) and protein S (PS) from *Physarum polycephalum* and *Myxococcus xanthus* or the yeast-killer toxin WmKT from *Williopsis mrakii* and a proteinase inhibitor from *Streptomyces nigrescens* SMPI have shown that they all share some structural characteristics with βγ-crystallins from vertebrate eye lens (Blundell et al., 1981; Bax et al., 1990; Jaenicke, 1999). A double Greek key motif was found to be the common topological theme, with the number and orientation of domains or the state of oligomerization as variations (Antuch et al., 1996; Rosinke et al., 1997; Bagby et al., 1994a,b, 1998; Ohno et al., 1998; Wenk et al., 1999; Clout et al., 2001). Although the βγ-crystallins and their microbial homologs S3a and PS were predicted to form similar structures, sharing a characteristic signature sequence (Wistow et al., 1985; Wistow, 1990), the killer toxin and proteinase inhibitor only showed remnants of this sequence fingerprint. One common feature of these representative examples is their high intrinsic stability. It allows the eye lens to grow thoughout life, maintaining transparency without significant turnover of its densely packed proteins. As typical stress proteins, S3a and PS from phylogenetically unrelated microorganisms share the anomalous stability of their eye-lens prototypes, with additional increments of stabilization coming from Ca^{2+}-ions as extrinsic factors (Kretschmar et al., 1999a,b; Wenk et al., 1999; Wenk and Jaenicke, 1999). One characteristic of domains comprising exclusively of Greek key motifs is that they always

contain two such motifs and are quite rare in comparison with, for example, β-barrel domains with the immunoglobulin-fold, which comprise only one complete Greek-key motif. In considering the structure-stability relationship of crystallins and their homologs it is interesting to note that the domain organization may involve both intra- and intermolecular interactions. Within the βγ-crystallin superfamily this distinctive characteristic has become obvious from three sets of experiments: first, altering either the conformation of the connecting peptide or the interface between domains changes both the mode of domain interactions and the mechanism of folding; second, the length of domain extensions at the N- or C-terminal ends of the polypeptide chain as well as removal of the termini may cause altered states of association; third, circular permutants with reverse order of domains may show significant changes in their physical characteristics and domain assembly (cf. Trinkl et al., 1994; Norledge et al., 1996, 1997b; Wright et al., 1998; Wieligmann, 2000).

In the following, we review our present understanding of the relationship between the structure, stability, and function of βγ-crystallins and their microbial homologs. As one would expect for structural homologs of widely different origin, there is a high degree of uncertainty with respect to their functional relationship. Regarding the anomalously high stability, certain predictions may be based on the common topological characteristics, bearing in mind the caveat that "traffic rules of protein stability" are still not in hand (Privalov, 1992; Murphy, 1995; Jaenicke and Böhm, 1998). Similarly, describing protein function is ambiguous, considering that proteins have at least the three-fold requirements or purposes of (1) folding to the native state, (2) performing one or several specific functions or biological roles (e.g., as "structural proteins" or "enzyme-crystallins"), and (3) degradation, serving as building blocks in either metabolism or translation, thus allowing continuous turnover and biosynthesis (Wetlaufer, 1980). With this premise, we shall focus this review on available experimental data on the structure, folding and stability of crystallins, rather than function, with the aim of applying the fundamental questions of protein structure and stability to the underlying mechanisms of physiological stress and cataractogenesis.

II. TOPOLOGY AND HIERARCHY

A. Greek Keys and Domains

Four adjacent antiparallel β-strands arranged in a pattern similar to the course of the Maiandros river in ancient Lydia represent a common secondary structural motif called a Greek-key, well known from Attic vases (Figure 1a); it is the most frequent naturally occurring topology of all possible arrangements of two sequentially adjacent hairpin motifs (Branden and Tooze, 1998). There are two classes observed in natural proteins: the Greek key as exemplified in the extensive Ig-fold family that occurs singly as part of a β-barrel, and the βγ-crystallin Greek key, which occurs in duplicate. This double Greek key represents the common feature in βγ-crystallins from eye lens as well as S3a, PS, SMPI, and WmKT from *Physarum*, *Myxococcus, Streptomyces,* and yeast (Jaenicke, 1999)

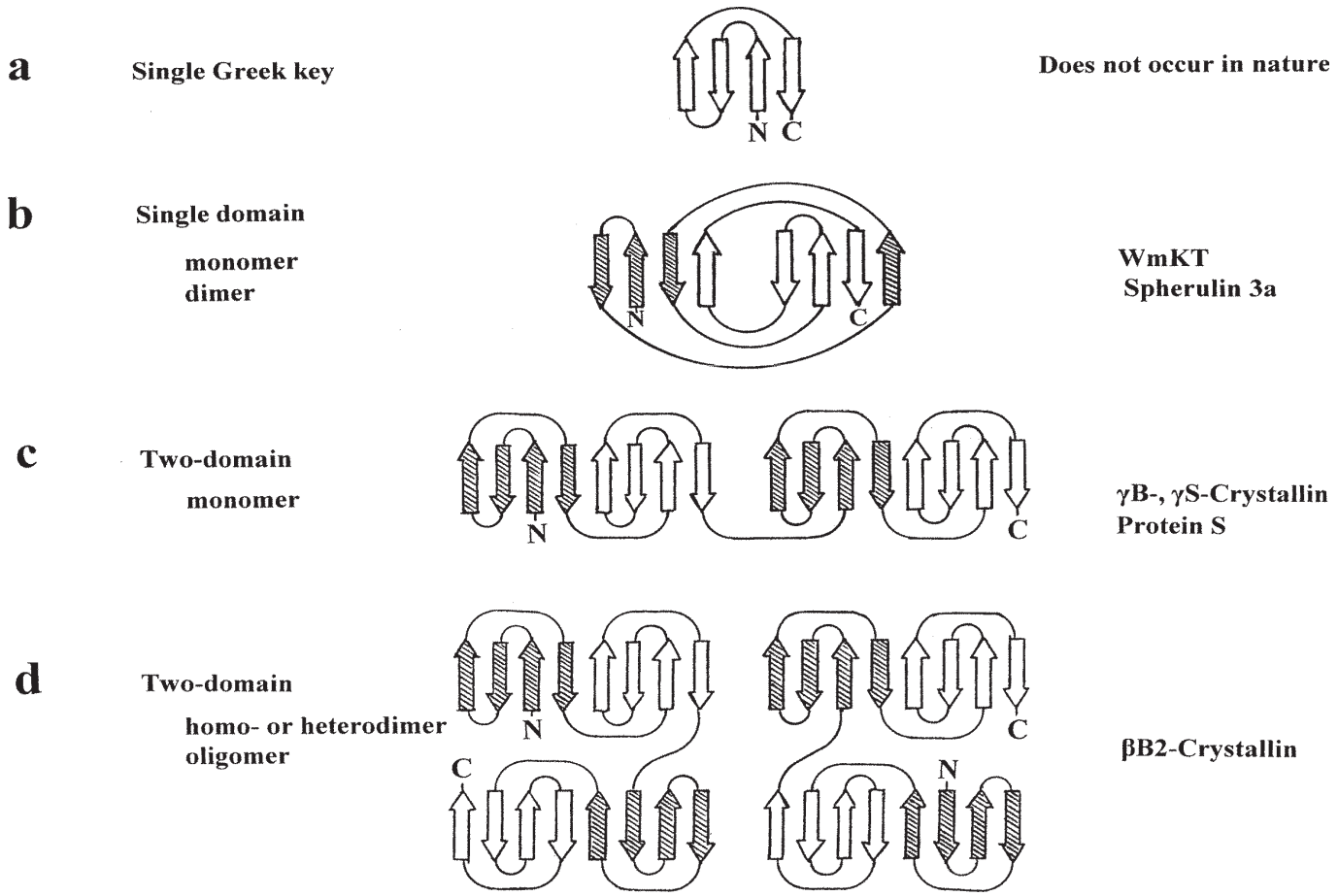

FIGURE 1. Hierarchy of proteins with the βγ-crystallin fold as multiples of Greek-key motifs. (**a**) 1 Greek key with 4 β-strands. (**b**) 2 intercalating Greek keys form a single domain with two β-sheets. The four consecutive β-strands of the first Greek key in each domain are called **a, b, c, d** in this review. Note how the first β-sheet is comprised mainly of the Greek key (**a, b, d**) shown in dark with the c strand donated from the second Greek key (shown in light). The dark and light motifs have different characteristics (see Figure 2) and the order of dark/light is permuted in Protein S. (**c**) 4 Greek keys form a two-domain monomer. In γ-crystallins, the pseudo-symmetric interface that binds domains involves interactions between topologically equivalent motifs (light Greek keys), whereas in Protein S the nonsymmetric interface involves the second (light) and third (dark) motifs. (**d**) 2 × 2-domain monomer domain swaps to form a dimer. The interfaces that bind the dimer together are between the light motifs in the top row and between the light motifs in the bottom row.

(Figure 1b). Sequence-structure alignment of all the Greek-key motifs shows that two quite distal residues, a glycine and a serine, are the most conserved and are involved in stabilizing the supersecondary fold by packing a β-hairpin over a β-sheet (Figure 2) (Blundell et al., 1981). Because these residues were only conserved in one of the Greek-key motifs of the SMPI and WmKT structures, they were not recognized as having this topology by sequence search tools. γB-Crystallin, the best-known member of the βγ-crystallin superfamily, is a highly symmetrical single-chain two-domain protein of 174 amino acid residues (Figure 2). The two domains show 37% sequence identity, which explains the high similarity of their tertiary fold (with 1.4 Å rms distances of the superimposed C_α atoms). Drawing the single strands as arrows, it becomes obvious that in each of the compact modules the polypeptide backbone consists of two separate β-sheets combining strands 2, 1, 4, 7 and 6, 5, 8, 3 (b, a, d, c´ and b´, a´, d´, c) to form a distorted barrel (Figure 1c and 2b). Thus, for the complete two-domain protein we end up with the schematical representation given in Figure 1c. From the point of view of evolution, the above homology considerations support the idea that the two-domain protein arose from a single-domain ancestor. Furthermore, the two Greek-key motifs within a domain show 3D similarity and a lower sequence identity than corresponding motifs between domains. This is consistent with a more ancient duplication from a single primordial gene coding for just one motif that has subsequently duplicated twice to yield the complete gene for present day vertebrate γB (Blundell et al., 1981). The organization of the β-crystallin gene, with its three introns between the four motifs, supports this hypothesis (Wistow and Piatigorsky, 1988). However, there are no introns between motifs in the γ-crystallin domains (Lubsen et al., 1988), which has implications for the one-domain/two-domain nature of the βγ-crystallin ancestor.

As indicated, the Greek-key motif in a single βγ-crystallin domain or in crystallin homologs always occurs in duplicate. Attempts to construct subdomains made use of the single-domain spherulin 3a from *Physarum polycephalum*. The expression of the recombinant N- and C-terminal half-molecules (single Greek-key motifs) of S3a was unsuccessful due to aggregation and/or misfolding and subsequent degradation of the truncated protein (Kretschmar, 1999). This suggests either of two possibilities: (1) a single Greek-key motif cannot dimerize to form a perfectly symmetrical βγ-crystallin-like domain and requires a covalent connection; (2) because the putative primordial one-motif gene duplicated and the protein products dimerized, the two halves of the molecule have diverged to be mutually complementary with a consequent reduction in symmetry preventing domain recreation from only one or other of the motifs. It is certainly the case that the double Greek key domain has a complex topology and folding mechanism with an obvious asymmetry in that only one tyrosine corner is present (Figure 2) (Hemmingsen et al., 1994; Clout et al., 2001). When the structure is viewed in terms of the two β-sheets forming a β-sandwich or a β-barrel, there are many connections (arches) that cross from one sheet to another and, unlike the jelly roll motif, cannot be conceptualized as folding from a single long β-hairpin (Branden and Tooze, 1998). What is special about the double Greek key domain topology is that each linear

a

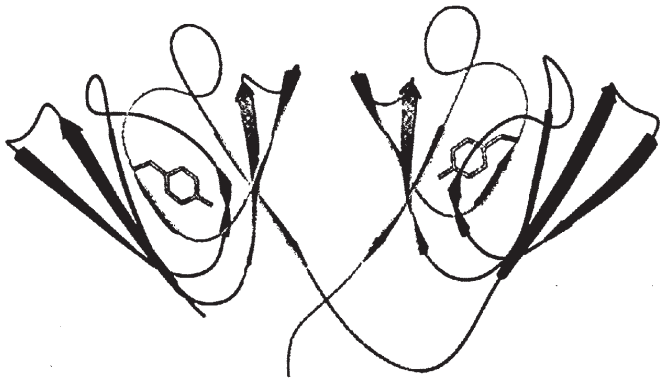

b

```
m1       1 GKITFYEDRGFQGHCYECSS-DCPNLQP-Y--FS-RCNSIRVDS  39
m3      88 FRMRIYERDDFRGQMSEITD-DCPSLQDRFH-LT-EVHSLNVLE 128
            ------      -----    -                ------

              *           *                          *
m2      40 GCWMLYERPNYQGHQYFLRRGDYPDYQQ-WMGFNDSIRSCRLI   81
m4     129 GSWVLYEMPSYRGRQYLLRPGEYRRYLD-WGAMNAKVGSLRRV  170
            ------      -----  ---                -----
              a           b     c                  d

cp      82 PQHTGT 87

c-arm  171 MDFY  174
```

FIGURE 2. Topology of the N- and C-domains of γB-crystallin. (**a**) A ribbon diagram of γB-crystallin showing the organization of four Greek keys, with motifs 1 and 2 forming the N-terminal domain (left) and motifs 3 and 4 the C-terminal domain. The two Greek-key motifs within a domain intercalate to form 2 β-sheets such that the **a, b, d** strands of one motif hydrogen bond with the c strand from the partner motif within each domain (cf. Figure 1b). Motifs 1 and 3 are shown in dark and largely form the outer solvent facing sheets, whereas the sheets that pack together about the domain interface are formed largely from motifs 2 and 4 and are shown in light (cf. Figure 1c). The two domains are joined by a linker or connecting peptide, and there is a short C-terminal extension or arm. The two domains are organized about a vertical approximate two-fold axis. The two appended tyrosine side chains are those of the tyrosine corners and are underlined in 2b. Note that each domain comprises one such corner. (**b**) The sequence of bovine γB-crystallin arranged to show the structural modules: motifs, connecting peptides (cp), and C-terminal arm. In the structurally aligned motif sequences, the conserved sequence signature of Y6 E7 F11 G13 S34 from motif 1 and topological equivalents are highlighted. The residues between the a and b strands of each motif form a highly conserved "folded β-hairpin" structure. The motifs are clustered into their similar pairs (1 + 3) and (2 + 4) in line with the more recent duplication of domains compared with ancestral motifs. The hydrophobic residues that pack together at the domain interface are labeled with * in motifs 2 and 4, and are shown in green in Plate 4a. The residues underlined in motifs 2 and 4 are the conserved G and Y of the tyrosine corners.

4-stranded motif exchanges its third β-strand to a β-sheet belonging to its partner motif, an essentially cooperative act (Figure 1b). This theme of mutual exchange is seen at higher levels of the complex hierarchy of crystallins (Figure 1d) (Bax et al., 1990). It may also occur in α-crystallin based on its sequence similarity to the small heat shock protein family that has been shown to comprise an Ig-fold that associates to higher oligomers through β-strand exchange (Kim et al., 1998).

As has been summarized in Figure 1, the double Greek key fold can occur as a single domain monomer, such as killer toxin, a single domain that is an obligate dimer, such as S3a, as two domain monomers as in γ-crystallins, or as two domain protomers that form obligate oligomers as in β-crystallins. In the following, the characteristics of this hierarchy is discussed in some detail.

B. Monomeric Single-Domain Constructs

There are no monomeric single-domain eye lens crystallins in nature. Thus, in order to investigate their properties, single N- and C-terminal domains of bovine γB-, bovine, and human γS-crystallin as well as domains of protein S from *Myxococcus xanthus* were produced either by limited proteolysis (Rudolph et al., 1990; Sharma et al., 1990) or by DNA technology, using *E. coli* as a host (Mayr et al., 1994; Wenk et al., 1999, 2000). The proteolyzed and the recombinant domains were isolated in pure form and characterized with respect to their physicochemical properties. X-ray crystallography and NMR analysis proved their spatial structure to be identical with the corresponding topological units in the complete proteins. As a representative example, Plate 1* summarizes the results for bovine γB-crystallin. The underlying diffraction data provide four pieces of information: (1) The two halves of the complete two-domain structure show a close structural relationship; (2) separation of the two domains from each other does not alter the backbone structure of the polypeptide chain significantly, differences in the C-domain refer to the C-terminal extension (Mayr, 1995; Norledge et al., 1996); (3) slight modifications, e.g., truncation of the C-domain, may cause structural alterations at the quaternary level providing insight into the evolution of multidomain proteins (Norledge et al., 1996); (4) depending on the packing of the domain interface and the tightness of specific interactions, isolated single domains may form nicked native-like assembly structures, in spite of the relatively low "local concentration" of the domains (Jaenicke, 1999; Wenk et al., 2000).

1. Yeast-Killer Toxin WmKT

WmKT from *Williopsis mrakii* is an 88-residue monomeric single-domain 9.5-kDa polypeptide that is secreted by the yeast to kill competing strains by blocking the β-glucan synthesis (Yamamoto et al., 1986). The protein is stable over the whole pH range between pH 2 and 11 and tolerates temperatures up to 100°C, at least for short periods of time, unlike the γ-crystallins that aggregate irreversibly around 75°C. In common with the 3D structure of γB-crystallin, the

* Plates appear following page 490.

topology of the protein is dominated by two Greek-key motifs, each consisting of four β-strands forming two twisted 4-stranded antiparallel β-sheets (cf. Plate 2*). The space between the two β-sheets is packed with hydrophobic side chains forming a central hydrophobic core (Antuch et al., 1996). At this point, WmKT shows a significant mechanistic difference from cytoplasmic eye-lens crystallins, which, under the reducing conditions in the cytoplasm, contain exclusively cysteine residues and no cystine bridges. In contrast, the toxin (as a secreted protein) requires a network of disulfide bonds to stabilize the single-domain as a monomeric entity. The respective cystine bridges crosslink hairpins in each of the two β-sheets; in addition, they anchor the two sheets against each other, and tie two loops together to form the regular secondary structure. Although γB and WmKT have the same topology or fold group, it is less clear that they are evolutionarily related. As taken from both sequence identity and spatially equivalent domain core packing residues, the βγ-crystallins are more closely related to a domain found in prokaryotes than they are to the aforementioned yeast fold (Clout et al., 1997). It is possible that, like the numerous examples of unrelated superfamilies with the Ig-fold, the WmKT and the βγ-crystallin folds are an example of convergent evolution. What is certainly the case here is that the same topology is associated with high intrinsic stability.

2. Spherulin 3a

Spherulin 3a (S3a), a Ca^{2+}-binding dormancy protein from the slime mold *Physarum polycephalum* showing ca. 22% sequence identity with the N-terminal domain of γB, is considered to be a member of the βγ-crystallin superfamily and thus represents the only known *bona fide* single-domain member. Under adverse environmental conditions, such as starvation, desiccation, cooling or exposure to heavy metal ions, multinucleate plasmodia of the slime mold sporulate to cryptobiotic oligonucleate microcysts (spherules), which are viable over long periods of time (Dove and Rusch, 1980). Spherulation has been shown to be accompanied by the biosynthesis of copious amounts of S3a and (to a lower extent) a small number of other cytosolic proteins, altogether of not fully understood biological function (Bernier et al., 1987).

S3a has been cloned and expressed as recombinant protein in *E. coli*. In its native form, the 103 residue single-domain polypeptide chain forms a stable dimer of 22-kDa molecular mass. Due to its exposed cysteine residue (C4), in the absence of reducing agents, intermolecular disulfide exchange causes covalent cross-linking to tetramers, octamers, and even higher polymers (cf. Section III.D.1, Table 3). In order to avoid these side reactions, the C4S mutant was produced. Being indistinguishable from the wild-type protein in all its physical properties, it was used to compare the stability of S3a with γB-crystallin. The results confirmed the expected close similarity of the bacterial protein with the domains of γB (Kretschmar et al., 1999a,b). Despite the relatively high molecular mass of the stable dimer, homo- and heteronuclear NMR spectroscopy was applied successfully to solve the three-dimensional solution structure of the Ca^{2+}-loaded protein

* Plates appear following page 490.

(Plate 3*). Only few, if any, intermolecular NOEs between the monomers were detected; line-width broadening was attributed to unspecific aggregation. As a result, the structure of the S3a monomer was described in terms of two pleated β-sheets, plus a short α helix, arranged into the γ-crystallin fold; the β-sheets comprise two intertwined Greek-key motifs (as in γB), with an additional N-terminal β-strand unique to S3a (Rosinke et al., 1997). The lack of intermolecular NOEs between the monomers suggested that the oligomerization does not involve extended subunit interfaces. Despite that, no concentration-dependent dissociation of the dimer was observed by ultracentrifugal analysis, indicating an anomalous mechanism of dimerization (Kretschmar et al., 1999b). However, the high-resolution X-ray crystal structure does show a dimer that exhibits twofold symmetry and is held together by an extensive interface (Figure 3) (Clout et al., 2001). Significantly, the nature of the domain-pairing interface was quite distinct from that found in the eye lens βγ-crystallin superfamily, indicating that this eukaryotic protein was not the direct ancestor of the crystallin domain pairs. However, the domain comprised a pair of twofold symmetric calcium binding sites that were very similar to those found in the N-terminal domain of the prokaryotic protein S (Wenk et al., 1999), thus further supporting the membership of S3a to the βγ-crystallin fold family.

C. Monomeric Two-Domain Crystallins

In proceeding to the next higher level in the hierarchy, the previous topological considerations with respect to domains still hold. For γB-crystallin as the prototype of a two-domain single-chain protein, they have been described before (cf. Section II.A). What is new is the *linker,* that is, the connecting peptide between the domains (Plate 4*): On the one hand, its length (determining the *local concentration* of neighboring structural entities) affects their interdomain interactions (Jaenicke, 1999; Wenk et al., 2000), and on the other, its conformation may cause oligomerization due to *domain swapping* (Bax et al., 1990; Bennett et al., 1995; Schlunegger et al., 1997).

1. γB- and γS-Crystallin

There are seven genes coding for γ-crystallins in mammalian lenses; other vertebrates may have more or less, not orthologous to the mammalian ones. As summarized in Table 1, the actual number of proteins synthesized and their relative amount vary with the species. Their expression patterns and solubility properties appear to be correlated with the decreasing refractive index gradient from the center to the cortex of the adult lens (Siezen et al., 1988; Slingsby et al., 1997). γB-crystallin is the major core crystallin in bovine lens and in the lenses of a number of other vertebrates, whereas γD- and γS-crystallin are the main structural eye lens proteins in rat and in humans, respectively (Lubsen et al., 1988; Lampi et al., 1997). Obviously, the amount and composition of the γ-fractions is variable between species, correlating with the lens properties. γB may be considered as the prototype of the βγ-crystallin superfamily. In contrast to γB, whose two-domain 3D structure is

FIGURE 3. The high-resolution X-ray structure of calcium-loaded spherulin 3a. (**a**) The crystal structure shows that two monomers form a dimer with 2-fold symmetric pairing between identical domains of S3a viewed down the dyad axis, which is not in the same plane as the intra-domain pseudo-two-folds relating motifs. By contrast, in the β- and γ-crystallins, the pseudo-two-folds that relate N- and C-domains and motifs within each domain are approximately planar (cf. Figure 2a). The two pairs of calcium atoms are shown as black circles. (**b**) The two domains are organized about a vertical approximate 2-fold axis with the interface filled with hydrophobic side chains.

TABLE 1
Complete Sequences for the Bovine and Human γ-Crystallin Families

Gene/protein	Old protein name	SwissProt ID	GenBank ID	PDB
Bovine				
γA √	Fraction IV	€	€	nd
γB √	Fraction II	P02526	117460	1AMM
γC X	-	¶	¶	nd
γD √	Fraction IIIb	P08209	2815497	1 ELP
γE √	Fraction IIIa	ø	ø	nd
γF √	Fraction IV	P23005	3334461	1A45
γS √	β_s	P06504	117419	1A7H ♯
Human				
γA √	-	P11844	117457	nd
γB √	-	P07316	117461	nd
γC √	-	P07315	117464	nd
γD √	-	P07320	2506321	‡
γE (pseudogene)				
γF (pseudogene)				
γS √	-	P22914	4033688	1HA4 ♯

√ protein detected in lens.

X protein not detected in lens.

€ not in database but sequences printed in Slinsby & Croft, 1978.

¶ not in database but sequence of γC printed in Hay et al., 1994.

ø not in database but sequence of γE printed in Norledge et al., 1997a.

♯ C-terminal domain only.

‡ The 3D structure of a cataract point mutation, R36S, has been solved (Kmoch et al., 2000), but the coordinates have not been deposited.

nd not determined.

known at atomic resolution (see Section IIA), so far the determination of the 3D structure of γS has been unsuccessful. Only the C-terminal domain of bovine γS has been solved by X-ray crystallography (Basak et al., 1998). Thus, an attempt was made to predict the structure by homology modeling, based on the close phylogenetic relationship of the two proteins. The model predicts that γS, apart from a 5-residue extension, differs from γB mainly in the interface region between the domains, including the linker region, which is one residue longer in γS-crystallin. The charged residues are paired in a different way from the parental structure, which may be correlated with their specific differences in solvation, phase separation, and stability (Zarina et al., 1994; Cooper et al., 1994a,b; Liu et al., 1996).

2. Protein S

Protein S (PS), the spore-coat forming protein of the soil bacterium *Myxococcus xanthus*, is structurally related to γB-crystallin (19% sequence identity, 47% similarity (see Wistow et al., 1985). After stress, the protein is expressed up to a level of ≈15% of the total cellular protein. Lysis of the peripheral cells of the syncytium leads to the release of PS, which polymerizes to a stable cuticula, this way allowing the dormant myxospores to endure cryptobiosis over long periods of desiccation or other types of stress (Kaiser et al., 1979).

NMR studies have shown that PS is a monomeric Ca^{2+}-binding two-domain protein of 173 amino acid residues, with each domain comprised of two similar Greek-key motifs, and a short α-helix (Plate 5a*) (Bagby et al., 1994a,b,c). Compared with the lens βγ-crystallins, the Greek-key motifs are permuted (Clout et al., 2001). The two domains are connected by a short linker peptide. As in γB, the domains form an intramolecular interface, but it is non-symmetric and hence quite different from both the βγ-crystallin and the S3a domain-pairing interfaces. In contrast to γB-crystallin, which undergoes irreversible aggregation after thermal unfolding, PS folds reversibly and therefore may serve as a model in characterizing the thermodynamic properties of simple two-domain eye-lens crystallins such as γB.

PS and its isolated domains, PS-N (A2→V89) and PS-C (M-Q90→S173-H_6), were expressed in *E. coli* and isolated as recombinant proteins, PS in authentic form according to its spectral and hydrodynamic properties (Wenk and Mayr, 1998; Wenk and Jaenicke, 1999). X-ray analysis of the isolated N-terminal domain allowed two Ca^{2+}-binding sites per domain to be localized (Plate 5b*) (Wenk et al., 1999). Remarkably, these binding sites are very similar to those observed in spherulin 3a (Clout et al., 2001). Removal of calcium by chelating agents such as EDTA leads to a destabilization of the protein (see below).

D. Dimeric Two-Domain Crystallins and Higher Oligomers

β-Crystallins comprise a multigene family of basic (βB1, βB2, βB3) and acidic (βA1, βA2, βA3, and βA4) polypeptides (Berbers et al., 1984, Lampi et al., 1997). The sequences of their corresponding globular domains exhibit

between 45 and 60% identity with each other, and about 30% with γ-crystallins (cf. Figure 2 and Plate 4c). Based on this finding, both β-crystallins and γ-crystallins are put together in a superfamily, with γ-crystallins as single-chain members, and the various β-crystallins as dimers and higher oligomers. The main sequence difference is that β-crystallins have N-terminal extensions compared with γ-crystallins, with the basic β-crystallins having in addition C-terminal extensions. βB2 forms a dimer in solution but shows versatility in its interactions as it may equally assemble with acidic and basic subunits, leading to heterodimers and higher mixed oligomers (Bindels et al., 1981, 1983a,b; Berbers et al., 1982; Slingsby and Bateman, 1990).

The crystal structure of bovine βB2-crystallin focused attention on the linker peptide between the N- and C-terminal domains, and away from the extensions. These were not visualized in the electron density (Bax et al., 1990), were observed to be flexible by 2D NMR (Carver et al., 1993a,b 1994; Cooper et al., 1993, 1994a,b, 1998), and consequently were judged not to be involved in stabilizing the dimer interface. As has been depicted in Plate 4a and 4b, the close spatial relationship between γB- and βB2-crystallin is clearly confirmed by comparing the high-resolution X-ray structures of the two proteins. The N- and C-terminal domains are clearly superimposable, and in both cases, the domain pairing exhibits pseudo-two-fold symmetry. The distinction between the proteins derives mainly from the linker conformation: In the 21-kDa γB monomer, the V-shaped connecting peptide allows intramolecular domain interactions, whereas in βB2-crystallin the linker is straight, thus favoring quaternary interactions between the dumbbell shaped 21-kDa subunits (Plate 4*). As a consequence of the topological similarity of the β- and γ-domains, their interactions are analogous, except for their *inter*molecular and *intra*molecular character. In βB2-crystallin the two subunits are related by a crystallographic dyad (P) interface. This transition from tertiary to quaternary interactions gives an idea how oligomers may have evolved from precursor monomers by using a domain interface either within one and the same polypeptide chain or between two of them (Bax et al., 1990). 3D domain swapping has been proposed as a general mechanism for forming oligomeric proteins from their monomeric forms (Bennett et al., 1994, 1995; Schlunegger et al., 1997), with additional stability being gained in a second step through the evolution of a new interface. 3D domain swapping in the β-crystallin example appears to be at the first stage, as the swapped domains are kept at "arms length" by their extended linkers.

It is possible that larger numbers of domains could assemble using the same equivalent interface but with the organization of higher point group symmetry. Such an assembly has been proposed for the six-domain AIM1 molecule whereby domain swapping has been used to build three sets of domain pairs related by an approximate threefold (P) axis (Ray et al., 1997). In native bovine lens βB2-crystallin, at the high protein concentration of the crystal lattice, the dimers associate to a tetramer about two further orthogonal dyads (Q and R). This leads to the deployment of yet more distinct areas of the domain surfaces being buried at twofold symmetry-related sites forming a closed dimer-dimer oligomer

* Plates appear following page 490.

with 222 symmetry (Bax et al., 1990; Lapatto et al., 1991; Norledge et al., 1997a). In contrast with these closed assemblies, it has been suggested that 3D domain swapping could lead to endless open-ended oligomers that would scatter light (Bennett et al., 1994).

Protein engineering suggested that extensions might affect higher organization. In fact, truncated βB2 variants lacking extensions ($\beta B2\Delta_{NC}$) and mutants with their linkers exchanged ($\gamma B\text{-}L_{\beta B2}$ and $\beta B2\text{-}L_{\gamma B}$) proved that both the N- and C-terminal extensions and the connecting peptides are essential for the quaternary structure of βB2 (Plate 4c). The two linker mutants are monomeric, whereas the truncation mutants were found to form dimers and tetramers (not interconvertible without denaturation). The spectral properties of the mutants resemble those of wild-type βB2, indicating that the overall fold of the subunits remains unaltered. Evidently, the sequence of the connecting peptide is critical for βB2 dimerization, whereas the N- and C-terminal extensions seem to serve as spacers preventing the formation of higher homo-oligomers (Trinkl et al., 1994; Norledge et al., 1997b).

Considering the isolated domains, protein engineering experiments provided evidence that sequence extensions can also influence the state of association of domain pairs. For example, in the case of γB, neither homodimers nor γB-like heterodimers of the isolated domains are detectable (Mayr et al., 1997); obviously, the domain interactions in the intact two-domain protein require the high local concentrations defined by the short linker peptide. However, the complete C-terminal domain (with its four-residue C-terminal extension) forms heterologous interactions with other domains leading to the solvent exposure of the natural interface (Plate 1b) with a subsequent dramatic loss in protein solubility from ca. 500 to < 10 mg/ml. At the limit of solubility misassembly due to wrong domain interactions leads to aggregation, precipitation and sometimes crystallization (Norledge et al., 1996). On the other hand, the C-terminal domain, truncated by just the C-terminal tyrosine residue, does form a symmetrical homodimer of domains in the crystal lattice, thus demonstrating that the interface region of the C-domain is complementary to itself (Plate 1c). The correct dimerization is inhibited by the C-terminal tyrosine alone (Norledge et al., 1996). In the case of β-crystallins, a gene fusion event is proposed to have turned a C-terminal extension into a linker. This is based on the observation that the two domains within a βB2 subunit are not in close contact, whereas there are strong interactions between domains from partner subunits that include the C-terminal extension (Plate 4b).

E. Multimers: α-Crystallins and "Crystallin Polymers"

α-Crystallins (αCs) are essential eye lens components. Despite their name, they are not limited to the eye lens, but also play an active role in cell protection and development. Sharing the homologous C-terminal *α-crystallin domain* of ~100 residues with the family of the ubiquitous small heat-shock proteins (Ingolia and Craig, 1982; de Jong et al., 1998), they serve as molecular chaperones, showing exceedingly high binding capacity with up to one substrate protein per subunit (Jaenicke and Creighton, 1993; Merck et al.,

1993; Jaenicke, 1996a; Beissinger and Buchner, 1998; Ehrnsperger et al., 1998; Horwitz et al., 1999; Ganea and Harding, 2000; Clark and Muchowski, 2000). With this function, they are assumed to be involved in maintaining lens transparency by preventing aggregation of misfolded or damaged proteins in the crowded fiber cells (Horwitz, 1992). There is evidence that ATP enhances the function of αC as a molecular chaperone (Muchowski et al., 1999; Wang and Spector, 2000). Accounting for up to 50% of the protein mass *in situ*, αC would prevent opalescence of the eye lens over a long period of time; only after "titrating out" the chaperone would the concentration of irreversibly denatured protein rise to the critical concentration at which aggregation occurs (Jaenicke and Creighton, 1993; Goldberg et al., 1991; Jaenicke and Seckler, 1997; Welch et al., 1998; Beissinger et al., 1999; Thirumalai and Lorimer, 2001).

There are two human α-crystallin genes, αA and αB, encoding 173 and 175 amino acid residues and sharing close to 60% sequence identity (Bloemendal and de Jong, 1991). They form polydisperse multimers with molecular masses between 300 and 1200 kDa, depending on the solvent conditions and other variables. Due to the polydisperse size distribution of both the natural and recombinant protein, crystallization of vertebrate α-crystallin has been unsuccessful so far. Thus, presently neither the detailed 3D structure of the αC subunit nor the topology of the subunit assembly are known. CD- and IR-based secondary structure predictions for the αC subunit suggested predominantly β-sheet and less than 20% helix content. Regarding the tertiary fold of the subunit, sequence comparisons between different β-sheet proteins led to the proposal that the αC domain might resemble an Ig fold (Tardieu et al., 1992). This hypothesis was confirmed with the high-resolution crystal structure of an archaeal 16.5-kDa sHsp, which furthermore showed that the 24-mer was built up from a dimer (Kim et al., 1998). Systematic site-directed spin labeling of α-crystallin is also consistent with this fold topology for the monomer, but indicates a different dimerization motif (Koteiche and Mchaourab, 1999).

In connection with the functionally relevant quaternary structure of αC, a number of models have been proposed, based on hydrodynamic data and subunit exchange, as well as light scattering, X-ray small-angle scattering, cryo-electron microscopy, image reconstruction, and homology modeling (Groenen et al., 1982; Tardieu and Delaye, 1988; Horwitz et al., 1998; Haley et al., 1998; Abgar et al., 2000). There seems to be general agreement that under physiological conditions the assembly process is characterized by a relatively fast subunit exchange, indicating a certain degree of conformational flexibility of the αC protomers (Tardieu and Delaye, 1988; Bova et al., 1997; Haley et al., 1998; Ehrnsperger et al., 1998; Abgar et al., 2000; Vanhoudt et al., 2000; Datta and Rao, 2000; Reddy et al., 2000). Classification of cryo-electron micrographs and 3D image reconstruction showed that the assembly consists mainly of protein shells of ~19 nm diameter with a central cavity ~8 nm in diameter. Both the intrinsic dynamics and variable subunit packing cause disorder so that the shells are not completely defined, and a certain percentage of the cavities seem to be open to the surrounding environment, with gaps or regions of weak density in the protein shell (Haley et al., 1998).

Relating this model to chaperone models that assume substrate seclusion within an *Anfinsen cage*, there are obvious differences, especially with respect to the conformational variability and polydispersity of the assembly structure (Beissinger and Buchner, 1998; Saibil, 2000). It may well be that exactly these characteristics are essential for a molecular chaperone in the crowded environment of the eye lens. The dynamic assembly characteristics and the high substrate binding capacity of the chaperone seem to be of utmost importance in preventing or delaying cataract formation (Horwitz, 1992; Raman et al., 1995; Haley et al., 1998; Horwitz et al., 1998, 1999; Derham and Harding, 1999; MacRae, 2000; Clark and Muchowski, 2000).

III. INTRINSIC AND EXTRINSIC STABILITY

A. Physical Basis of Protein stability

The stability of proteins refers to either covalent and noncovalent conformational changes. For covalent reactions responsible for irreversible protein denaturation see Ledl and Schleicher (1990), Volkin et al. (1995), Jaenicke (2000). Noncovalent denaturation is not necessarily reversible, especially in the case of modular or oligomeric proteins, which are prone to aggregation and coagulation due to the wrong interdomain or intersubunit interactions as side-reactions on the folding/association pathway (Jaenicke and Seckler, 1997). To quantify the thermodynamic stability of a given protein, the transition from the native (N) to the denatured (U) state needs to be complete and fully reversible (Tanford, 1968, 1970; Privalov, 1979, 1982, 1992; Pfeil, 1981, 1998; Pace, 1986; Makhatadze and Privalov, 1995; Pace and Scholtz, 1997). If both requirements are fulfilled, the $N \Leftrightarrow U$ equilibrium transition allows the free energy of stabilization to be calculated. For small, monomeric, single-domain proteins, which usually undergo fully reversible unfolding transitions, the analysis is straightforward. However, for more complex domain or oligomeric proteins, this is not the case. Therefore, considering the anomalous long-term stability and the complexity of αβγ-crystallins, it is essential to briefly discuss what stability means and how it is determined.

The free energy of conformational stability of a globular protein is defined as the difference between the free energies of the folded and the unfolded states

$$\Delta G_{stab} = G_{unfolded} - G_{native} \qquad (1a)$$

The corresponding expression for the enthalpy change

$$\Delta H_{stab} = H_{unfolded} - H_{native} \qquad (1b)$$

is essential because ΔH_{stab} can be determined either directly from calorimetric experiments (ΔH_{cal}) or from a van't Hoff plot ($\Delta H_{van't\ Hoff}$), that is, from the temperature dependence of the apparent equilibrium constant K of the transition

$$N \overset{K}{\Leftrightarrow} U \qquad (2)$$

Comparing the results of both approaches allows the "two-state assumption" in Eq. 2 to be tested: if only N and U and no intermediates are populated in

the transition, ΔH_{cal} equals $\Delta H_{van't\ Hoff}$, otherwise $\Delta H_{cal}/\Delta H_{van't\ Hoff}$ is > 1 (Privalov, 1979; Jaenicke, 1991). A qualitative standard criterion to test the two-state model is to compare the equilibrium transitions monitored by different spectral properties or by biological activity as a function of temperature, pH, or denaturant concentration. If the profiles do not coincide, intermediates are present in significant amounts so that one equilibrium constant is not sufficient to quantify the denaturation process. In cases where the reaction does obey Eq. 2, the thermodynamic stability in terms of the free energy of unfolding can be calculated from the equilibrium constant K according to

$$\Delta G_{stab} = -RT \ln K \qquad (3)$$

with R = gas constant and T = absolute temperature. Under physiological conditions, that is, in water at constant pH, pressure, and temperature (pH 7, 1 bar, 25°C), the changes in Gibbs free energy as 1 mol of reactant is converted to 1 mol of product represents the *standard Gibbs free energy change* $\Delta G^{\circ\prime}$. Given the high molecular mass of proteins and their relatively high partial volume, molar concentrations are experimentally inaccessible; thus, in order to compare the stabilities of proteins, their free energies have to be normalized, for example, to millimolar or micromolar concentrations. In the case of oligomeric proteins such as spherulin (S3a), reversible denaturation is commonly accompanied by dissociation. Accordingly, Eq. 2 needs to be converted into

$$N_2 \overset{K_D}{\Leftrightarrow} 2U \qquad (4)$$

Because of mass action here, the equilibrium of unfolding/dissociation K_D depends on the monomer concentration:

$$K_D = [U]^2/[N_2] = 2[M]\ (f_U^2/(1-f_U) \qquad (5)$$

with [M] = molar monomer concentration and f_U = fraction of denatured protein. In contrast to the dimensionless equilibrium constant K in Eq. 3 for a monomeric protein, K_D has the dimension of a concentration. Normalization to 1 m*M* concentration, ΔG at 25°C is shifted by 17 kJ/mol (Thompson et al., 1993; Neet and Timm, 1994; Mok et al., 1996; Gloss and Matthews, 1997).

As one would expect, the above equilibrium constants K and K_D depend on the denaturation conditions, because in a given experiment different variables may be superimposed in the destabilization of a protein. For example, in the case of γB-crystallin, neither low pH nor urea alone were able to denature the protein; only the combination of pH 2 and high urea concentration allowed the unfolded state to be reached. Similarly, numerous hyperthermophile proteins only "melt" beyond the boiling point of water; thus, in order to shift the temperature of thermal unfolding (T_m) down to a manageable range, low pH or low concentrations of chaotropic agents (urea or guanidinium chloride) are required (Figure 4a) (Jaenicke and Böhm, 2001). Aiming at the conformational stability as *free energy under standard conditions*, the nonphysiological denaturing conditions need to be corrected by extrapolating the experimental ΔG_{stab} data to zero denaturant concentrations (at 25°C, pH 7). With this approach, $\Delta G_{stab}^{\circ\prime}$ values are obtained that allow different proteins to be compared with respect to their free energies of stabilization (Pace, 1986; Pace and Scholtz, 1997). Because of the significant temperature dependence of the enthalpy (ΔH) and entropy (ΔS) of globular proteins in aqueous

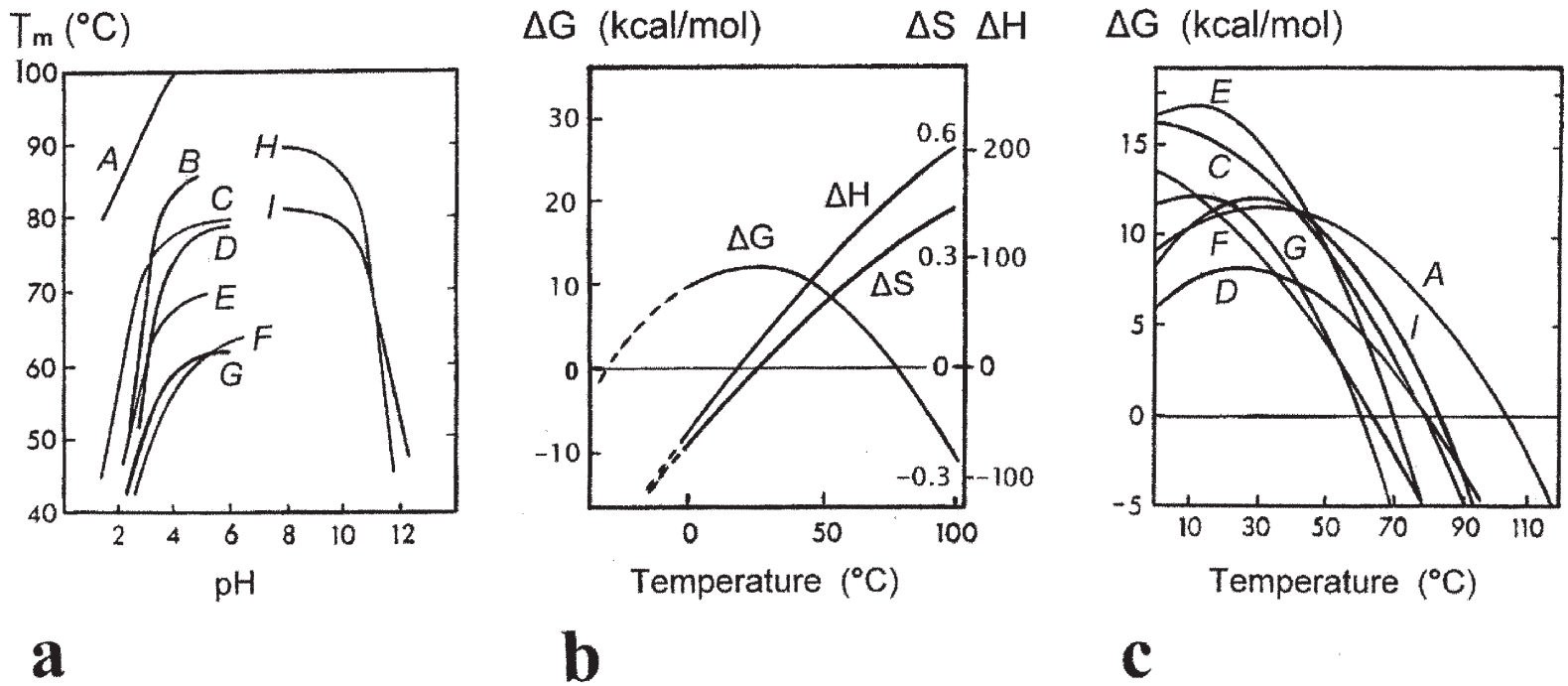

FIGURE 4. Energetics of protein structure (cf. Privalov, 1979; Jaenicke, 1991). (**a**) pH dependence of the denaturation temperature (T_m) of selected globular proteins, illustrating the superposition of heat denaturation and electrostatic destabilization: *A* = basic pancreatic trypsin inhibitor; *B* = papain; *C* = hen lysozyme; *D* = ferricytochrome c, *E* = trypsin; *F* = ribonuclease A; *G* = α-chymotrypsin; *H* = parvalbumin ($+Ca^{2+}$); *I* = metmyoglobin. (**b**) Enthalpy, entropy, and Gibbs free energy of the thermal unfolding of myoglobin. ΔH and ΔG are given in kcal/mol, ΔS in kcal/(K × mol). Due to the temperature dependence of ΔH and ΔS, the temperature profile of ΔG is parabolic, with a maximum at ambient temperature and two N⇔U equilibrium transitions at low and high temperature (*cold-* and *heat denaturation*) (Jaenicke, 1990; Privalov, 1992; Franks, 1995). (**c**) Free energy of stabilization of globular proteins at pH values close to their optimum stability; alphabetical references to the respective proteins as in **a**. Compared with standard proteins from mesophiles, ultrastable proteins, for example, from hyperthermophiles show maximum values around 30 to 40 kcal/mol (120 to 160 kJ/mol). Thus, commonly mesophilic and extremophilic homologs differ by no more than the equivalent of a few weak interactions (Grättinger et al., 1998; Dams and Jaenicke, 1999; Jaenicke and Böhm, 2001).

solution, the ΔG vs. T profiles observed for the thermal unfolding of proteins exhibit parabolic characteristics (Figure 4b); their maxima cluster in a narrow range between 30 and 80 kJ/mol (7 to 20 kcal/mol) (Figure 4c); other modes of denaturation such as guanidinium chloride, urea, or pH give the same result, provided they are corrected to standard conditions (Makhatadze and Privalov, 1995; Pfeil, 1998). Thus, despite the large number of noncovalent contacts maintaining the native structure of proteins, the Gibbs free-energy change after protein dissociation and unfolding is minute. Compared to the total molecular energy of a protein (~ 10^7 kcal/mol for a small protein of 100 amino acid residues, cf. Baldwin and Eisenberg, 1987), it represents a small difference between large numbers originating from the compensating contributions of attractive and repulsive forces to the close packing and the minimization of hydrophobic surface area characteristic for globular proteins in their native state. Commonly, ΔG_{stab} corresponds to no more than a couple of hydrogen bonds or hydrophobic interactions, or to just a few ion pairs, this way allowing the functionally important compromise between rigidity (stability), on the one hand, and flexibility (folding/function/degradation) on the other (Baldwin and Eisenberg, 1987; Huber, 1988; Dill, 1990; Jaenicke, 1991; Shirley et al., 1992; Pace et al., 1996; Schellman, 1997). Obvious differences in ΔG_{stab} are attributable to the different purposes of proteins; for example, structural proteins need to be more stable than protein hormones or enzymes involved in metabolic regulation. Evidently, crystallins belong to the first category; still, their free energy of stabilization does not exceed the above range significantly, bearing in mind that a small change in net charge or binding a ligand may double the free energy of stabilization (Kretschmar and Jaenicke, 1999; Wenk and Jaenicke, 1999; Wenk et al., 2000).

For the sake of clarity, it needs to be kept in mind that protein denaturation is rarely fully reversible so that determining thermodynamic stability may be difficult or even impossible. Therefore, frequently *relative* stabilities have been used to characterize proteins, especially if homologs from different species or wild-type and mutant proteins were compared. To give the rank order of stability, in these cases commonly the onset of thermal unfolding or deactivation (T_m or T_M), or the denaturant concentration at the $N \rightarrow U$ transition midpoint ($c_{1/2,urea}$, $c_{1/2,GdmCl}$) is used, ignoring reversibility. Especially for multidomain and multisubunit proteins or complex assembly systems, this approach has often been the only means to obtain at least qualitative data.

The fact that proteins exist close to the borderline of denaturation does not allow general strategies of protein stabilization to be formulated (Dill, 1990; Matthews, 1993, 1996; Böhm and Jaenicke, 1994). As a state function, ΔG_{stab} is additive. Increments come from compact packing of the hydrophobic core (minimization of cavity volume), high levels of secondary structure (α-helix content, extended β-structures, helix-capping) (Pace et al., 1996; Auerbach et al., 1998), hydrogen-bond networks (Cooper, 2000), ion-pair clusters (Perutz and Raidt, 1975; Yip et al., 1998), replacement of conformationally strained residues by glycine, oligomerization (Jaenicke, 1991; Murphy, 1995; Jaenicke et al., 1996; Thornton, 2001; Jaenicke and Böhm, 2001). The given enthalpic stability increments may be supplemented by entropic contributions due to

either water release accompanying the burial of ionized and nonpolar sites (Kauzmann, 1959; Jaenicke and Lauffer, 1969; Lauffer, 1975; Baldwin and Eisenberg, 1987; Jaenicke, 1987), or lowering the unfolding entropy by proline substitution or by the deletion of loops (Suzuki, 1989, 1992; Thompson and Eisenberg, 1999), or due to the decrease in rotational and translational degrees of freedom after quaternary structure formation (Doty and Myers, 1953; Tanford, 1973; Jaenicke, 1987; Janin, 1995; Makhatadze and Privalov, 1995; Tamura and Privalov, 1997; Auerbach et al., 1998; Dams et al., 2000).

Apart from the difference in the free energy levels of the native and denatured states according to the above two-state equilibrium (Eq. 2), activation barriers along the $N \rightarrow U$ unfolding pathway may govern protein stability in terms of *kinetic stabilization*. Here, increased intrinsic stability is attributable to a decrease in the rate of unfolding due to a high *free energy of activation* ($\Delta G^{\ddagger}_{N \rightarrow U}$) rather than *Gibbs free energy* (ΔG_{stab}) (Tomschy et al., 1994; Pappenberger et al., 1997; Cavagnero et al., 1998; Ogasahara et al., 1998). The 7-kDa single-domain all-β cold-shock protein (CSP) from *Bacillus subtilis* (thermal denaturation at T_m = 52°C), *Bacillus caldolyticus* (T_m = 72°C) and *Thermotoga maritima* (T_m = 90°C) may serve as an example. Measuring the unfolding and folding kinetics of the three proteins, the rates of thermal *unfolding* were found to be strongly decreased with increasing T_m, clearly reflecting the evolutionary requirements in the widely differing natural habitats of the three bacteria. In contrast, *folding* occurred at closely similar high rates (τ = 1.0 ± 0.2 ms), despite numerous sequence variations among the three proteins. In the given cellular context this means that in all three cases the nascent polypeptide chain is quickly protected against covalent and noncovalent denaturing effects due to the extremely fast formation of the compact native structure. For a detailed analysis see Perl et al. (1998, 2000).

As mentioned, folding/unfolding transitions (according to Eq. 2) do not necessarily show full reversibility; if irreversible consecutive reactions occur, the overall kinetics may be modeled by

$$N \underset{k_{I \rightarrow N}}{\overset{k_{N \rightarrow I}}{\Leftrightarrow}} I \xrightarrow{k_{I \rightarrow U}} U \qquad (6)$$

with I as a partially unfolded intermediate and $k_{N \rightarrow I}$, $k_{I \rightarrow N}$ and $k_{I \rightarrow U}$ as rate constants for the respective reversible and irreversible transitions. The observed rate of the overall process $k_{obs} = (k_{N \rightarrow I} \cdot k_{I \rightarrow U}) / (k_{I \rightarrow N} + k_{I \rightarrow U})$ is determined by the rate of partial unfolding ($k_{N \rightarrow I}$), as only I undergoes irreversible denaturation to U. Obviously, for the long-term stability of eye lens crystallins, that is, lens transparency, the kinetic stability of N is highly significant, because low unfolding rates under physiological conditions keep the level of unfolded protein low, this way minimizing irreversible processes such as chemical modification and aggregation.

Considering the viscosity of highly concentrated proteins, one might expect that the native state of crystallins *in situ* may also be favored by friction-dependent kinetic stabilization. In fact, protein folding/unfolding has been reported to be viscosity dependent (Ansari et al., 1992; Kern, 1992; Jacob et al., 1997; Plaxco and Baker, 1998; Bieri et al., 1999; Bieri and Kiefhaber, 1999). In the corresponding *in vitro* experiments it is not easy to separate frictional effects

from the extrinsic stabilization in the presence of viscogenic components such as sucrose, glycerol, polyethylene glycol, or complex multicomponent systems. However, performing experiments at constant protein stability clearly indicated that both the rates of unfolding and folding are effected by the viscosity of the solvent (Jacob, 2000). From these model studies we conclude that in the fiber cells of the eye lens, as in the seeds of plants (E.E. Hood, P. Lillford, P. Walstra, personal communication), the high protein levels enhance protein stability.

Single protein components taken out of the cell and purified to homogeneity have often been found to exhibit drastic destabilization compared to their *in vivo* characteristics. Apart from the above friction-dependent kinetic stabilization, at this point extrinsic stabilizing factors of low molecular weight as well as *compatible solutes* need to be considered. Any specific ligand of a given protein, ions, coenzymes, substrates, etc. may serve as extrinsic factor (Jaenicke, 1999, 2000). Typical compatible solvent components are proline, betaine, glycerol, or other polyhydric compounds. Their stabilizing effects are linked to the preferential hydration of proteins in the presence of the "structure-making" solvent components, due to nonspecific interactions related to the perturbation of the solvent structure in contact with the protein surface. The predominant mechanism is an increase in the surface tension of water by the osmolyte. By opposing the increase in hydrophobic surface area this favors the native state because, for a globular protein in aqueous solution, unfolding necessarily exposes hydro-phobic groups from the interior into the outside medium. This situation is thermodynamically unfavorable; thus, the system reacts by maintaining a minimal total protein-solvent interface, corresponding to maximal hydration and a deficiency of cosolvent in the protein surface (Franks et al., 1990; Timasheff, 1992; Carpenter et al., 1993; Jaenicke, 1996a,b; Timasheff and Arakawa, 1997; Knapp et al., 1999).

B. Stability Increments in Eye-Lens Crystallins

The βγ-superfamily of eye lens crystallins and their microbial homologs are topologically similar, their domains are superimposable, and they occur in pairs. With the incremental nature of ΔG_{stab} in mind, comparing the stabilities of the monomeric or oligomeric single- and multi-domain variants, one might expect a steady increase in stability in going from monomeric single domains (e.g., spherulin 3a) to domain pairs (such as protein S and γB-crystallin), further to βB2-crystallin as a four-domain dimer, and finally to higher oligomers (cf. Jaenicke, 1991). Experimental data in Figure 5 proves the prediction to be incorrect, both quantitatively and qualitatively: βB2 is less stable than γB, mainly due to the lower intrinsic stability of the isolated domains, and the quaternary structure is effected in an unpredictable way when altering the linker peptides or the N- and C-terminal extensions. Evidently, no general strategies of stabilization can be extracted, even from closely related proteins belonging to one and the same topological family. What may be gained from a systematic study of isolated domains and their interactions in two-domain and in oligomeric structures is some insight into the contributions to the intrinsic and extrinsic

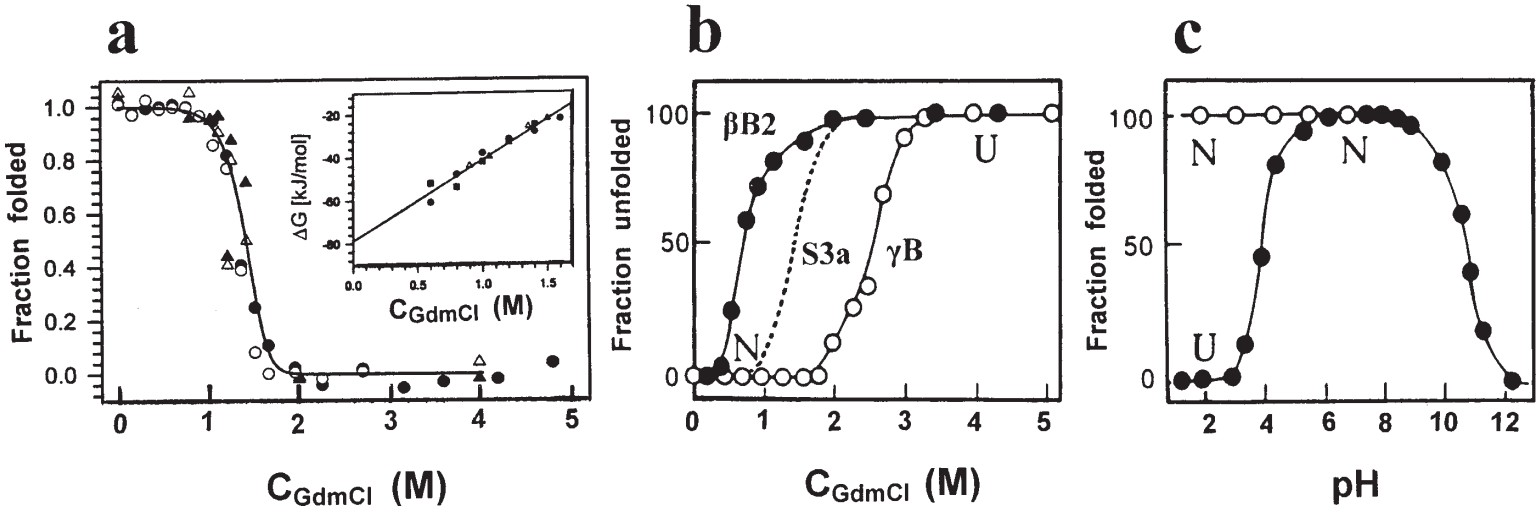

FIGURE 5. Unfolding transitions of *Physarum polycephalum* spherulin 3a, bovine γB-crystallin and rat βB2-crystallin. (**a**) GdmCl-dependent equilibrium unfolding of Ca^{2+}-free S3a C4S (c_{S3a} = 0.3 mg/ml in 25 m*M* Mops buffer pH 7.0) monitored by fluorescence emission at 360 nm (o), dichroic absorption at 213 nm (●), sedimentation coefficient (▲) and molecular mass from analytical ultracentrifugation (Δ). At 100-fold dilution (c_{S3a} = 3 μg/ml), the transitions are shifted downward by 0.4 *M* GdmCl. *Insert:* Extrapolation for zero denaturant concentration: $\Delta G_{GdmCl\ !i0}$ = 79 ± 6 kJ/mol (Data from Kretschmar, 1999). (**b**) GdmCl-dependent equilibrium unfolding of Ca^{2+}-free S3a (· · · ·), γB-crystallin (open symbols), and βB2-crystallin (closed symbols), monitored by maximum fluorescence emission in 0.1 *M* Na-phosphate pH 6.0 (Kretschmar, 1999; Jaenicke, 1999). (**c**) pH-induced unfolding of γB- (open symbols), and BB2-crystallin (closed symbols), monitored by 315 nm fluorescence emission in Gly/HCl, citrate/H_3PO_4, Tris/HCl and Gly/NaOH at 0.1 *M* ionic strength (Jaenicke, 1999).

stabilities at the various levels of the structural hierarchy of proteins. Considering the entire crystallin superfamily, the most important stabilizing factors seem to be (1) the accumulation of hydrogen bonds in antiparallel β-sheets (cf. Section II.A), and (2) the modular structure, with compact domains exhibiting mutual stabilization. Evidently, the latter effect depends on the close neighborhood and the complementarity of the domain interfaces, illustrating the significance of the local concentration of the modules (Jencks, 1969; Kirby, 1980). Extrinsic stabilization may be attributed to the ligand-induced tightening of domains or subunits (Durchschlag, 1986; Durchschlag et al., 1991; Groß and Jaenicke, 1994), apart from the previously mentioned effect of preferential solvation (Timasheff and Arakawa, 1997).

As one would predict from their polyelectrolyte nature, differences in net charge and alterations in preferential ion-binding will exhibit dramatic effects on the stability of proteins (Privalov, 1979). For example, in the case of intact γB-crystallin, urea denaturation can only be accomplished at pH 2, where widely separate equilibrium transitions of the two domains seem to indicate a dramatic difference in their intrinsic stabilities. At physiological pH, the effect vanishes. A plausible explanation is that complete protonation at pH 2 adds a strong electrostatic potential to the urea-induced destabilization (Privalov, 1979); at pH 7, both domains possess the same net charge, whereas at pH 2 they differ by 3 units. In the human eye lens, γS-crystallin replaces γB as the main component (Harding and Crabbe, 1984). Both proteins are highly homologous, although the charge distribution of their domains differs; in γS the maximum difference at low pH is only 1, compared to 3 in γB. As a consequence, in γS urea induces only a single two-state equilibrium transition with characteristics closely similar to those of the constituent domains, whereas γB shows bimodal unfolding characteristics (Wenk et al., 2000; see below). That charge compensation due to ion binding may alter the situation becomes clear from data obtained for spherulin 3a and protein S. In contrast to γB-crystallin, both proteins exhibit high-affinity Ca^{2+}-binding and, as a result, *extrinsic stabilization* by either formation of coordination complexes or preferential solvation (see Section III.D.1 and 2).

Considering intact γB-crystallin from calf eye lens, hydrodynamic and spectroscopic data have clearly shown that the monomeric two-domain protein preserves its native structure over the whole pH range between pH 1 and 10. In 0.1 *M* phosphate, at pH 7, the protein is stable up to 75°C and, even at pH 2, complete unfolding requires exceedingly high urea concentrations. Beyond the given limits, denaturation is only partially reversible so that thermodynamic data for the protein under standard conditions have not been obtained with satisfactory precision. At low pH, making use of sedimentation velocity, intrinsic fluorescence, circular dichroism and thermal analysis, the mechanism of the urea-dependent equilibrium unfolding was quantitatively analyzed in terms of a three-state mechanism

$$N \Leftrightarrow I \Leftrightarrow U \qquad (7)$$

The intermediate (I), with one domain unfolded and the other still intact, was found to be highly populated at 3 *M* urea and pH 2.0 (Figure 6a). Kinetic experiments, changing the solvent con-

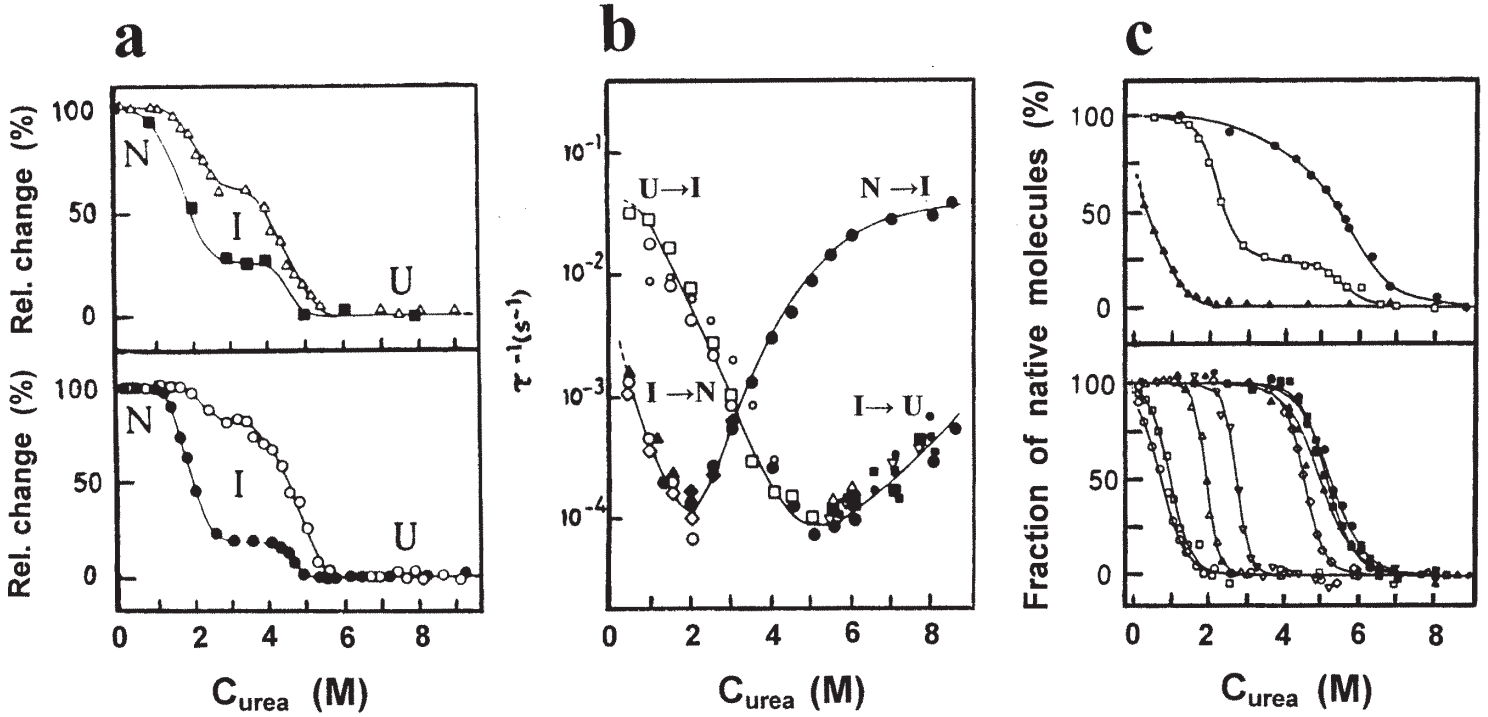

FIGURE 6. Urea-dependent equilibrium unfolding of bovine γB-crystallin and its isolated domains γB-N and γB-C (with permission, Rudolph et al., 1990; Mayr et al., 1997). (**a**) Three-state transition of intact γB (0.2 mg/ml in 0.1 *M* NaCl/HCl pH 2.0, 20°C), monitored by circular dichroism (Δ), sedimentation coefficient (■) (upper frame), and change in fluorescence emission at 360 nm (●) and 320 nm (○) (λ_{exc} = 280 nm) (lower frame). (**b**) Rates of unfolding/refolding at 0.2 mg/ml, in 0.1 M NaCl/HCl pH 2.0, 20°C, monitored by fluorescence emission of native γB at 360 nm (unfolding ●, folding ○), 320 nm (unfolding ■ , folding □), GPC/FPLC (unfolding ◆, folding ◇); fluorescence emission of intermediate (I) at 360 nm (unfolding ▲ folding Δ) and 320 nm (unfolding ∇). Fluorescence emission of γB-N at 360 nm (unfolding ●, folding ○) and 320 nm (unfolding ■); 1 μ*M* protein concentration, 20°C. (**c**) Comparison of intact γB and its isolated N-terminal (closed symbols) and C-terminal domains (open symbols). ***Upper frame:*** γB (□), γB-N (●), and γB-C (▲) in 0.1 *M* NaCl/HCl pH 2.0, 20°C, monitored by fluorescence emission. ***Lower frame:*** γB-N at pH 2.0 (▲), pH 3.0 (■), pH 4.0 (●); γB-C at pH 2.0 (○), pH 2.5 (□), pH 3.0 (Δ), pH 3.5 (∇), pH 4.0 (◇); 1 μ*M* protein concentration in 100 m*M* NaCl/HCl, Gly/HCl, and 60 m*M* formate buffer, 20°C.

ditions stepwise from N to I to U in both directions yielded two separate chevron profiles (for N ⇔ I and I ⇔ U), in accordance with Eq. 4, thus proving both the *equilibrium* and *kinetic* intermediates to be identical (Figure 6b) (Rudolph et al., 1990). To correlate the mechanism with the 3D structure of γB, the recombinant isolated N- and C-terminal domains (γB-N: 1-84, 1-87; γB-C: 87-173, 87-174), as well as the product of limited proteolysis (1–88) were studied, again comparing the urea denaturation profiles at pH 2. As a result, γB-C turned out to show only marginal stability, whereas γB-N showed the above I ⇔ U transition (Figure 6c, upper frame). γB-C (87–174) was crystallized as a separate entity, diffracting to a resolution of 1.55 Å; the solved structure had atomic coordinates isomorphous to the C-terminal half of the intact parent molecule (Plate 1a) (Norledge et al., 1996). However, crystallization and structure solution of the N-terminal domain, γB-N, was dependent on an interface mutation (Palme et al., 1998a). Modifying the hydrophobic core in the interdomain interface of the intact two-domain γB molecule, where M43, F56, I81, and the topologically related residues V132, L145, V170 make van der Waals contacts with each other (Plate 4a* cf. Jaenicke, 1996b), it becomes clear that at the given pH the mutual stabilization of the C-terminal domain comes from interdomain hydrophobic interactions. Nonconservative F56 mutants cause a destabilization of γB-C, whereas the stability of the γB-N is affected to a much lower extent (Table 2) (Palme et al., 1997, 1998b). $\Delta\Delta G_{stab}$ for γB-C amounts to –16 kJ/mol. Thus, at high net charge, the stability of the C-terminal domain of intact γB is dominated by its interactions with the N-terminal one; its intrinsic stability is only –4.7 kJ/mol (Mayr et al., 1997).

As mentioned, the low pH used in the above experiments with intact γB-crystallin was required in order to accomplish denaturation of the "ultrastable protein" (Rudolph et al., 1990; Jaenicke, 1996b). In the case of the isolated domains, less stringent pH conditions were found to be sufficient, clearly demonstrating that domain pairing contributes significantly to the stability of the two-domain monomer. On the other hand, the differential stability of the two domains γB-N and γB-C as a function of pH stresses the role of charge distribution to domain stability. For the γB-N domain, the transition midpoint of urea denaturation, $c_{1/2,urea}$, shows no significant pH dependence (5.0 ± 0.2 *M* at pH 2–4), whereas in the case of the γB-C domain the unfolding transition shifts from $c_{1/2,urea} < 1$ *M* at pH 2 to 4.5 *M* at pH 4 (Figure 6c, lower frame). This finding is in agreement with what one would expect from polyelectrolyte theory: Each of the two domains has an equal number of acidic and basic side chains; however, in γB-C, the total number is higher. At pH 7, both domains being close to their isoelectric point they do not differ significantly in their physicochemical characteristics; at pH 2, when all carboxylates are protonated, the net charge of γB-C exceeds that of γB-N by + 3, thus adding a significant electrostatic potential to the chaotropic destabilization (cf. Figure 4a).

γS-Crystallin, like the members of the γB-crystallin family, is a monomeric two-domain protein exhibiting close similarity to γB with respect to its gene organization and its sequence; however, it does not show the above bimodal unfolding characteristics under any condi-

* Plates appear following page 490.

TABLE 2
Molecular Characteristics of γB- and γS-Crystallin Variants [a]

Variant (Residues)	M_{calc} (Da)	M_{obs} (Da)	pH	z	T_m (°C)	ΔH (kJ/mol)	ΔG (kJ/mol)	ΔG* (kJ/g)	$c_{1/2,urea}$ (M)	$c_{1/2,GdmCl}$ (M)
Bovine γB-crystallin										
γB (1-174)	20965	**20700**	2.0	29			20.7		2.1 /5.1[b]	
γB-N (1-87)	10403	11100	2.0	13					5.0	
γB-C (87-174)	10692	11600	2.0	16					0.7	
γB (N+C)	21095	12000	2.0	29					0.7/5.1[b]	
γB-C (87-174)	10692	10750	2.0	16			4.7±0.2		0.70	
γB-C (87-174)			2.5	15			7.3±0.5		0.95	
γB-C (87-174)			3.0	14			25.5±1.6		1.95	
γB-C (87-174)			3.5	12			34.8±2.6		2.75	
γB-C (87-174)			4.0	9			36.0±1.9		4.50	
Bovine γB-crystallin mutants [c]										
γB (WT)	20965	20800	2.0	29					2.1/5.1[b]	
γB (F56W)	21005	21500	2.0	29					1.5/4.0[b,d]	
γB (F56A)	20890	20200	2.0	29					1.0/4.0[b,d]	
γB (F56D)	20934	-	2.0	~29					0.8/4.0[b,d]	
γB (R79E)	20939	20500	2.0	~28					2.0/4.0[b,d]	
CP-$γB_{(87-174)-L-(1-84)}$[e]	monomer		2.0	29					0.7/5.1[b]	
$γB-L_{βB2}$	20960	22500	6.0	~1					2.1/5.1[b]	

TABLE 2 (continued)

Bovine γS-crystallin										
BγS (1-177)	20796	21400	7.0	~0					7.0	2.1
BγS-5 (6-177)	20362	20870	7.0	~0					7.4	2.1
BγS-N (1-91)	10513	10710	7.0	~0					6.6	1.8
BγS-C (93-177)	10174	10310	7.0	~0					6.0	1.6
BγS (N+C)	20687	15500[f]	7.0	~0						
Human γS-crystallin										
HγS (1-177)	20876	21500	7.0	~0	75±1	750±20	84±0	4.0±0.5	8.0	2.6
HγS-N (1-90)	10480	10990	7.0	~0	70±1	380±10	42±5	4.0±0.5	7.0	1.9
HγS-C (91-177)	10413	10710	7.0	~0	78±1	430±10	48±5	4.5±0.5	7.6	2.5
HγS (N+C)	20893	10180	7.0	~0						

a M_{calc},M_{obs}: molecular masses, calculated and taken from ultracentrifugal analysis; z: calculated net charge at given pH values; T_m, ΔH: calorimetrically measured temperature and enthalpy of denaturation; ΔG, ΔG^*: Gibbs free energy at 20°C (kJ/mol) and corrected for given molecular masses (J/g); $c_{1/2,urea}$, $c_{1/2,GdmCl}$: transition midpoints of urea and guanidinium chloride denaturation. Data from Jaenicke, 1999; Mayr et al., 1994, 1997; Palme et al., 1997, 1998a,b ; Wenk et al., 2000.

b Transition midpoints of urea denaturation for the C-/N-terminal domains of intact γB.

c M_{calc} and M_{obs} for the separate domains differ at most by 6 %.

d The isolated N-terminal domains of the mutants do not differ in $c_{1/2,urea}$. At z=0, γBN-(F56A) dimerizes with an orientation differing from the one in natural γβ-crystallins.

e Changing the length of the linker L from Gly_3 to Gly_5 has no effect on the stability.

f The sedimentation coefficients of the separate domains and their mixture differ by ~25 %.

tion (Wenk et al., 2000). To understand the structural correlates, γS and its domains were compared with γB and its corresponding fragments. The extensionless mutant (with the 5 N-terminal amino acids missing) was included, because it brings γS closer to γB, which lacks the extension. As has been mentioned, the 3D structure of the protein is still unknown. Making use of homology modeling (based on the X-ray coordinates of γ- and β-crystallin), it was suggested that γB and γS are distinct in the interface region between their domains (Zarina et al., 1994). Together with the above mentioned different charge distributions between the N- and C-terminal halves of the two proteins, this allows the different unfolding mechanisms at low pH to be explained: γB-C, due to its larger electrostatic potential unfolds prior to γB-N giving rise to independent bimodal unfolding characteristics (N ⇔ I ⇔ U), while γS obeys the two-state model (N⇔U). This holds for γS from bovine and human eye lens. In both cases intermediates with one domain unfolded and the other still intact could not be detected. This holds at temperatures up to 80°C over the whole pH range between pH 2 and 11.5, thus allowing the detailed quantitative evaluation of the thermodynamic properties of the protein (Wenk et al., 2000).

Making use of recombinant bovine and human γS and its isolated N- and C-terminal domains (γS-N and γS-C), chemically and thermally induced equilibrium unfolding experiments showed that in the case of the intact bovine protein at pH 7 the C-terminal domain is less stable than the N-terminal one, whereas for human γS, despite its high structural homology, the opposite holds true. Another difference between the two proteins is the tendency to form heterodimers of the isolated domains: the bovine protein forms "nicked γS" with K_{ass} ~ 3 m*M*, while the human protein shows a much lower association tendency (Wenk et al., 2000; cf. Table 1). Bearing the general discussion in Section III.1 in mind, it is not surprising that no rationale for these differences can be given. Even the detailed 3D structure would hardly provide a clear-cut explanation, considering that the known coordinates of the C-terminal domain of γS are in agreement with the topology of full-length γB (Basak et al., 1998).

In summarizing presently available data, γS- and γB-crystallin differ in their structurally and thermodynamically relevant characteristics at three levels: (1) the length of the connecting peptides, (2) the distribution of ion pairs in the surface of the two molecules, and (3) the interactions at the interfaces between the domains (Zarina et al., 1994; Mayr et al., 1997). In the case of γB, the latter do not allow the N⇔U equilibrium transition to be quantified (Palme et al., 1997; Mayr et al., 1997; Jaenicke, 1999). In contrast, for γS and its isolated domains the complete thermodynamic analysis was easily accessible using the simple two-state approach (Wenk et al., 2000). The results for both the bovine and human protein are summarized in Table 2 and Figure 7. The fact that there is no significant pH dependence has to do with the even charge distribution between γS-N and γS-C. With ΔG_{stab} = 84 kJ/mol, the Gibbs free energy of stabilization of the human protein is relatively high. Correcting the value for the molecular mass, ΔG_{stab} for the intact protein equals the corresponding data for the isolated domains, indicating that interactions between the domains do not contribute significantly to the overall stability of the protein, in contrast to the results obtained for γB and its F56 mutants.

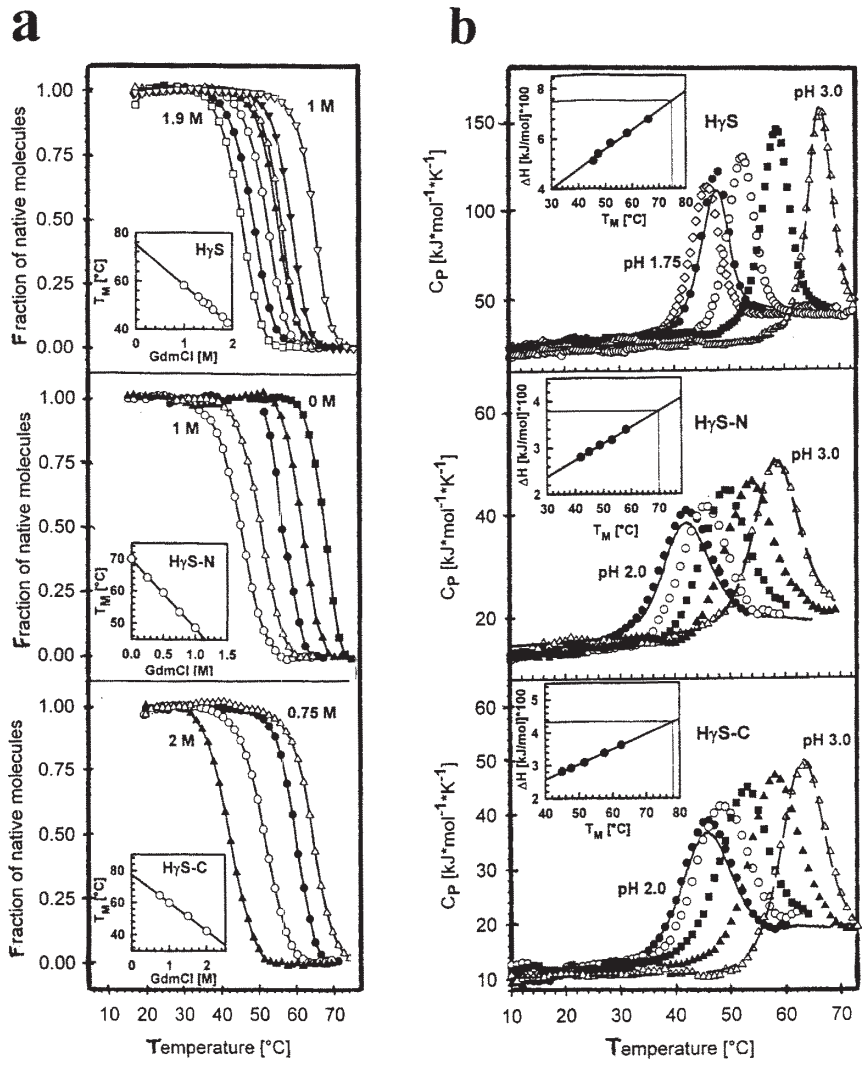

FIGURE 7. Thermodynamic stability of human γS-crystallin and its isolated domains HγS-N and HγS-C (with permission from Wenk et al., 2000). (**a**) Normalized thermal transitions of HγS (upper frame), HγS-N (middle frame), and HγS-C (lower frame) in phosphate buffer pH 7 at 50 μg/ml protein concentration and varying GdmCl concentration, monitored by absorbance at 286 nm. ***Inserts:*** T_M vs c_{GdmCl} plots with extrapolation to zero GdmCl concentration. (**b**) Calorimetric scans of HγS (upper frame), HγS-N (middle frame), and HγS-C (lower frame) at 0.8 to 1.5 mg/ml protein concentration and varying pH (glycine buffer pH 1.75 to 3.0). *Inserts:* Enthalpy vs T_M plots with linear regression for the calculation of ΔC_p and the determination of ΔH_M, using T_M at pH 7, extrapolated from thermal and GdmCl-induced unfolding transitions in a.

C. Implications of Domain Topology and Subunit Association

As has been mentioned, the two-domain structure of γB-crystallin does not allow a quantitative thermodynamic analysis due to undefined side reactions interfering with full reversibility. In the case of the dimeric βB2, reversibility of the unfolding/dissociation reaction can be easily accomplished; however, the concentration-dependent association step does not allow the two-state approximation to be applied for a quantitative ther-

modynamic evaluation (Dams and Jaenicke, 1999). γB and βB2 are distinct mainly by virtue of their linker peptides (cf. Plate 4). For γB, it was proposed that G86 in the interdomain region allows the polypeptide chain to change its direction into a V-shaped conformation, generating the stabilizing hydrophobic interface *between the domains*. In contrast, in βB2, the extended conformation of the linker favors *intersubunit* interactions, thus causing dimerization by domain swapping (Bax et al., 1990; Schlunegger et al., 1997). Exchanging the linker peptides by engineering the βB2- and γB-linkers ($L_{\beta B2}$ and $L_{\gamma B}$) between the γB- and βB2-domains challenges this explanation of the swapping hypothesis as both linker mutants are *monomeric* (Table 3). Evidently, in the case of γB, the domain interactions dominate the folding topology of both the wild-type protein and the γB-$L_{\beta B2}$ mutant so that the urea-induced equilibrium transitions of both proteins coincide. βB2-$L_{\gamma B}$, the alternative "transplant", shows only one single unfolding transition, despite its similarity with γB. As a monomer, it does not depend on protein concentration (in contrast to the dimeric wild-type protein) and shows only a slight shift to higher denaturant concentrations (Figure 8). The given findings allow two conclusions to be drawn: (1) the extended linker peptide is involved in the dimerization of βB2-crystallin, and (2) the stabilities of the native proteins reflect the intrinsic stabilities of the individual βγ-crystallin domains rather than the fold topology.

In this context, another feature of the βB2 subunit (again not present in γB) is the occurrence of terminal extensions protruding from the surface of the dumbbell-shaped monomers at both ends of their polypeptide chains. Evidence suggesting that they serve as "spacers" preventing the polymerization of βB2 beyond the dimer came from truncation mutants: eliminating the 15-residues N-terminal and the 12-residues C-terminal "arms", and expressing the recombinant protein ($\beta B2_{\Delta NC}$) in *E. coli* resulted in the overproduction of truncated 3.4S dimers and (to a lower extent) 5.3S tetramers. Subjecting the latter fraction to chemical denaturation/dissociation in urea, subsequent renaturation/reassociation yielded exclusively the homogeneous 3.4S species, proving that in free solution the dimer represents the most stable form of the protein (Trinkl et al., 1994). Comparing the X-ray structures of both forms, the mutant solution tetramer has a set of domain interactions very similar to the native lattice tetramer; however, the structures differ in the relative orientation of the two sets of four domains (Norledge et al., 1997b).

In following up the hypothesis that the linker between the domains and the extensions at the terminal ends determine the quaternary structure of βγ-crystallins, another series of experiments made use of circular permutants of the domains, that is, constructs with the N- and C-terminal domains linked inversely, and the original polypeptide chain clipped at any suitable position allowing a stable structure to be formed. In numerous cases, circularly permutated *CP-proteins* have been shown to possess native structure and function (cf. Jaenicke, 1999), proving that vectorial folding from the N- to the C-terminus is not a necessary requirement for correct folding. In order to design a suitable connector between the permuted domains, the correct domain boundaries were taken from the known 3D structures of γB and βB2. The proper choice of the clipping sites allows the local concentration and the correct interaction of the domains to be optimized.

TABLE 3
Molecular Characteristics of Rat βB2-Crystallin and βB2-Mutants [a]

βB2-variant	Residues	M_{calc} (kDa)	M_{obs} (kDa)	$s_{20,w}$ (S)	State of association	$c_{1/2,urea}$ (M)
βB2	205 (-16-185)	23.38	42.6±1.9	4.23	dimer	2.6[b]
βB2-N	107 (-16-88)	12.03	19.8±3.1	1.85	dimer[c]	1.2
βB2-C	99 (88-185)	11.64	10.6±1.0	1.21	monomer	2.9
$\beta B2\Delta_{NC}$	178 (-1-173)	20.50	38.5±2.5	3.42	dimer	1.7
$\beta B2\Delta_{NC}$	178 (-1-173)	20.50	72.2±2.8	5.34	tetramer	1.8
CP-βB2	176	20.13	39.5±1.8	3.34	dimer	2.2
$\beta B2\text{-}L_{\gamma B}$	(cf. Figure 2)	23.33	22.0±1.8	2.53	monomer	2.2
$\gamma B\text{-}L_{\beta B2}$		20.96	22.5±2.0	2.50	monomer	2.1/5.1[d]

a M_{calc} and M_{obs}: molecular masses, calculated and taken from ultracentrifugal analysis; $s_{20,w}$: sedimentations coefficient; state of association taken from ultracentrifugal analysis and gel permeation chromatography; $c_{1/2,urea}$: transition midpoints of urea denaturation. Data from Jaenicke, 1999; Mayr et al., 1994, 1997; Norledge et al., 1996, 1997a,b; Trinkl et al., 1994; Wieligmann, 2000; Wieligmann et al., 1998, 1999).

b Measurements in 0.1 M sodium phosphate pH 7.0 plus 0.3 M ammonium sulfate, 5 mM DTT and 2 mM EDTA. At ~ 5 μg/ml, βB2 exhibits concentration-dependent dissociation to partially unfolded monomers; at 200 μg/ml, the dimer-monomer transition shows enhanced cooperativity with $c_{1/2,urea} = 2.9\pm0.1$.

c At < 50μg/ml, dissociation to unfolded monomers according to $M_2 \Leftrightarrow 2I \Leftrightarrow 2U$.

d Transition midpoints for the C-/N-terminal domains of γB (cf. Table 1).

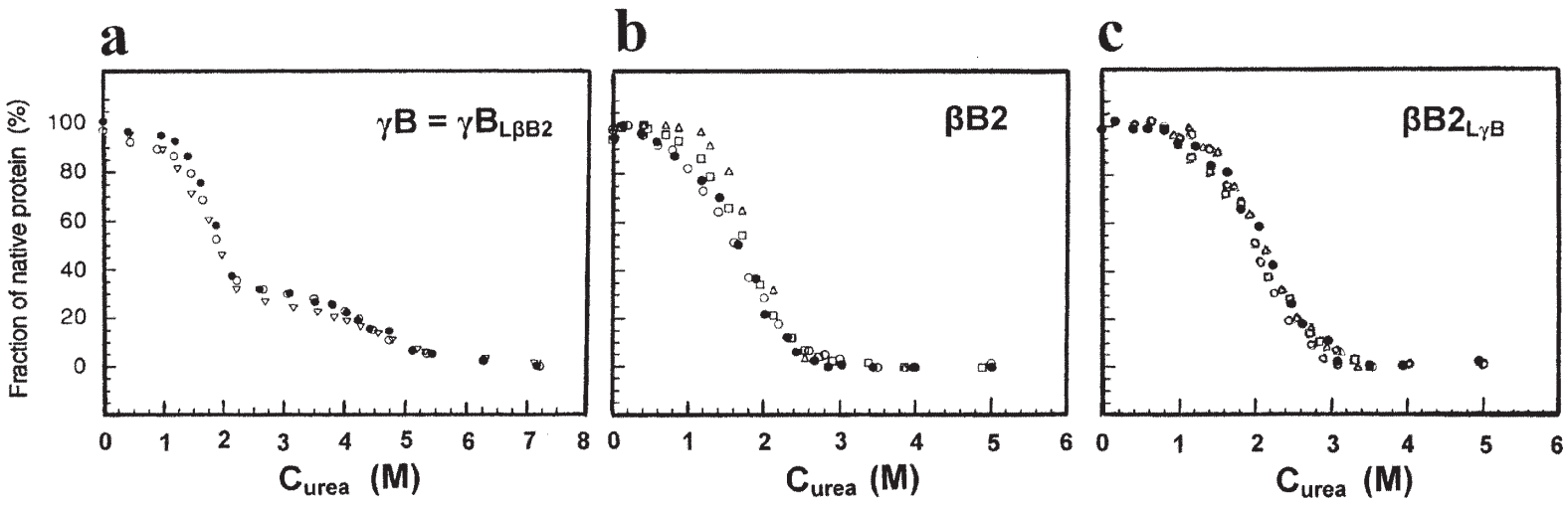

FIGURE 8. Urea-induced equilibrium unfolding of natural bovine γB-crystallin, rat βB2-crystallin, and their linker mutants $\gamma B_{L\beta B2}$ and $\beta B2_{L\gamma B}$ (Mayr et al., 1994; Trinkl et al., 1994). (**a**) Comparison of the unfolding transition of intact natural (∇) and recombinant (O) γB and its linker mutant $\gamma B_{L\beta B2}$ (●) at 20 μg/ml protein concentration, monitored by fluorescence emission (F_{320nm}/F_{358nm}) in 0.1 *M* NaCl/HCl buffer pH 2, 20°C. (**b**) Unfolding transitions of βB2 at varying protein concentration: Δ/□/o : unfolding at 200/20/4 μg/ml; ●: refolding at 4 μg/ml, monitored by fluorescence emission in 0.1 *M* phosphate buffer pH 7, 25°C. (**c**) Unfolding transition of $\beta B2_{L\gamma B}$ at Δ/□/o = 80/20/10 μg/ml; ●, refolding at 20 μg/ml; conditions as in b.

In the case of γB-crystallin, circular permutation was accomplished by deleting G86 in the original linker, and by changing T87 and T85 into the new N- and C-termini; triglycine and pentaglycine were inserted as connectors (cf. Table 2). Both constructs, CP-γB(G_3) and CP-γB(G_5), were found to be monomeric, showing identical equilibrium unfolding transitions, with no indication for hydrophobic docking of the domains, on the one hand, and no effects of the local domain concentration, on the other. Instead, the transitions resembled the superimposed transitions of the separate N- and C-terminal domains of the parent molecule (Mayr, 1995; Wieligmann, 1996, 2000). In designing the corresponding βB2-construct (CP-βB2), an attempt was made to mimic γB-crystallin by clipping the linker of the termini-truncated polypeptide followed by joining the new termini (residues 175 and –1). To avoid the destabilizing effect of a bulky residue at the point where the linker joins the second domain, W175 was replaced by G, leading altogether to the schematic CP-βB2 sequence

E 87…. I170—Linker—P1 …K 82
N^*-Domain C^*-Domain

with R171..Q174-G175-N-1 as linker

The protein formed a dimer in solution (Wieligmann et al., 1998) (Table 3). At first sight, this suggested that the intended γB-like topology was not realized. However, the crystal structure revealed that the native domain-swapped βB2 subunit had converted to intramolecular domain pairing on permutation (Wright et al., 1998). Surprisingly, the two γB-like monomers associate to form a dimer that resembles the top half of the native lattice tetramer (equivalent to the QR axes) (Plate 4). Urea- and temperature-induced denaturation transitions give evidence for a slight increase in stability, in keeping with the additional buried domain interfaces. However, $c_{1/2,urea}$ and T_m are in no way comparable with the extreme stability limits of γB, thus indicating that the stability in this case does not follow the topology and domain organization, but resides in the individual domains (Wieligmann et al., 1998, 1999).

D. Stability and Stabilization of Microbial Crystallins

1. Spherulin 3a

Spherulin 3a, the only known single-domain member of the βγ-crystallin superfamily, possesses a tertiary structure resembling the topology of γB-crystallin (see Section II.C.2), whereas the homodimeric quaternary structure is different. Due to its exposed cysteine residue (C4), in the absence of reducing agents intermolecular cystine bridges lead to the formation of higher oligomers. To address the question whether this side reaction effects the intrinsic stability of the protein, natural S3a was compared to the C4S mutant; both were found to be authentic with respect to their hydrodynamic and spectral properties (Kretschmar et al., 1999a). Despite the decrease in entropy of the denatured state, disulfide cross-linking has obviously no significant effect on the denaturation reaction (Mayr, 1995; Kretschmar et al., 1999a). In order to exclude irreversible perturbations of the two-state mechanism, in the following the cysteine-free C4S mutant will be considered.

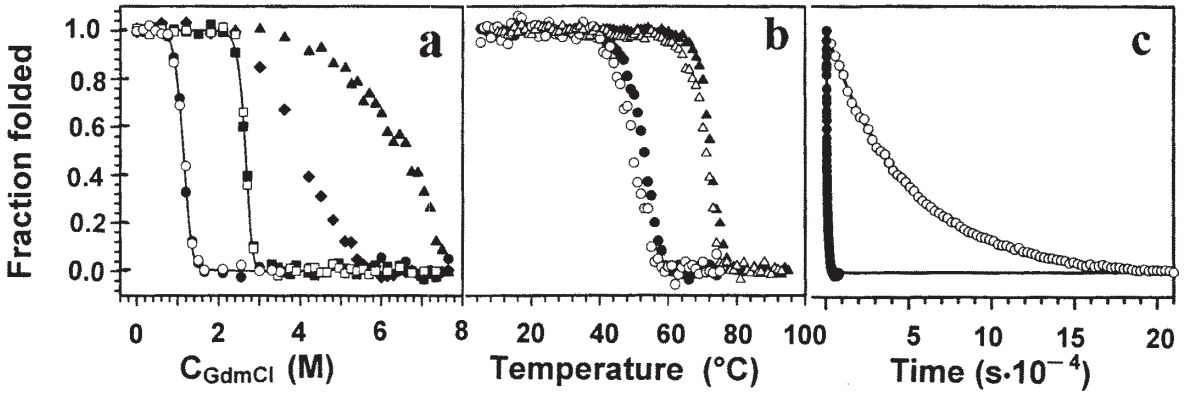

FIGURE 9. Thermodynamic and kinetic stability of spherulin 3a in 25 m*M* Mops buffer pH 7.0, in the absence and in the presence of Ca^{2+} (Kretschmar et al., 1999b). (**a**) GdmCl-induced equilibrium transitions of S3a (40 μg/ml), monitored by fluorescence emission at 25°C. Renaturation was started from the fully denatured protein (after 16 h in 6 *M* GdmCl). In the absence of Ca^{2+}, unfolding/refolding after 1 day (●/○); in the presence of 3 m*M* $CaCl_2$: unfolding after 2 days (▲), unfolding after 4 weeks (◆), and unfolding/ refolding after 8 weeks (■/□). (**b**) Temperature-induced equilibrium transition of S3a, monitored by dichroic absorption in the presence of 0.8 *M* GdmCl. Thermal denaturation was performed at 0.1 (open symbols) and 1.0 mg/ml protein concentration (closed symbols), either in the presence (△,▲) or in the absence of Ca^{2+} (○, ●). Ca^{2+}-binding and enhanced S3a concentration stabilize the protein, the latter due to the concentration-dependent shift of the monomer-dimer equilibrium to the native dimer. (**c**) Unfolding kinetics of S3a, monitored by fluorescence emission at 40 μg/ml. Kinetic traces at 2.5 M GdmCl for the Ca^{2+}-free protein (●), or at 7.5 *M* GdmCl for the Ca^{2+}-saturated protein (○). Using GdmSCN to accomplish full denaturation of Ca^{2+}-S3a, and extrapolating both the GdmSCN- and the GdmCl-dependent unfolding kinetics to zero denaturant concentration, the rate constants in the absence and in the presence of Ca^{2+} were found to be $6.1 \cdot 10^{-6}\ s^{-1}$ and $0.8 \cdot 10^{-6}\ s^{-1}$, respectively; thus, the the Ca^{2+}-saturated protein is kinetically stabilized, showing an eight-fold decrease in its unfolding rate.

TABLE 4
Molecular Characteristics of Spherulin 3a and S3a C4S [a]

Protein	Additive	M GPC (kDa)	M AUC (kDa)	n	$c_{1/2,GdmCl}$ (M)	T_m (°C)	ΔH_{cal} (kJ/mol)	ΔH_{vH} (kJ/mol)	$\Delta H_{vH}/\Delta H_{cal}$	ΔG^o (kJ/Mol)
Spherulin 3a										
	0.15 µM NaCl	22	21.2	2	1.2±0.1[b]	54[c]				
		38[d]	39.4	4						
		63,82[d]		6,8[d]						
	5 mM DTT	22	21.9	2						
Spherulin 3a C4S										
	0.15 µM NaCl	22	21.9	2	1.1±0.1	53.3[e]	523	546	1.05±0.05	81± 8
	3 mM $CaCl_2$	21.5	21.6	2	2.5±0.1	68.7[e]	1020	966	0.95±0.05	137±11

a M (GPC,AUC): Molecular mass determined by gel-permeation chromatography and analytical ultracentrifugation, respectively; n: state of association; $c_{1/2,GdmCl}$: transition midpoints of guanidinium-chloride denaturation; T_m, denaturation temperature; ΔH_{cal}: calorimetrically measured enthalpy of denaturation ΔH_{vH}, van´t Hoff enthalpy (kDa/mol dimer); $\Delta H_{vH}/\Delta H_{cal}$ ratio as two-state criterion; ΔG^o: Gibbs free energy at 25°C. Solvents: 25 mM MOPS buffer pH 7.0 and 25 mM cacodylate buffer pH 7.0, plus 1 mM EDTA ± 3 mM $CaCl^{2+}$. Maximum error: M_{GPC} 8%, M_{AUC} < 5%, T_m ±1.5°C, ΔH ±4%. Data from Kretschmar & Jaenicke, 1999; Kretschmar et al., 1999a,b).

b Reversible equilibrium transition as monitored by fluorescence emission, circular dichroism and sedimentation analysis at 300 µg/ml S3a concentration; at 10 µg/ml, the transition is shifted downward by 0.3 M GdmCl.

TABLE 4 (continued)

c Reversible equilibrium transition monitored by circular dichroism (θ_{213nm}) in the presence of 0.8 M GdmCl at 1.0-1,5 mg/ml; at 0.1 mg/ml, T_m is shifted downward by ~ 4°C.

d Gel-permeation chromatography allows cystine cross-linked dimers, tetramers, hexamers and octamers to be separated. High-speed sedimentation equilibria confirm the tetramer as the smallest component in the mixture.

e Extrapolated from chemically-induced equilibrium transitions at 1.0-3.0 M GdmCl, monitored by differential scanning calorimetry.

Calorimetric and spectroscopic analyses clearly show that S3a shares the high stability of its eye-lens homologs: In the absence of Ca^{2+}, its denaturation profiles range between those of γB- and βB2-crystallin, the tertiary structure being destabilized at pH < 4, the secondary structure at pH < 3. Guanidine- and temperature-induced denaturation occur at $c_{1/2,GdmCl}$ = 1.2 *M* and T_m = 54°C, respectively, both depending on concentration due to the dimeric state of the protein (Figure 5, Kretschmar et al., 1999a). Despite this concentration dependence (and in contrast to the βB2-dimer), thermal and chemical equilibrium unfolding transitions obey the two-state model according to $N_2 \Leftrightarrow 2$ U, allowing thermodynamic parameters to be determined (Table 4). As mentioned in Section III.A, this is by no means trivial. The Gibbs free energy of stabilization is 81 ± 8 kJ/mol, close to the above value for γS-crystallin. No significant differences were found between the free energies calculated from calorimetric enthalpies (ΔH_{cal}) and T_m; in addition, the free energy derived from thermal unfolding was confirmed by the spectroscopic results obtained from GdmCl-induced unfolding transitions at different temperatures (Kretschmar and Jaenicke, 1999).

Apart from the high *intrinsic* stability reflected by the aforementioned high Gibbs free energy, there are two further contributions that still enhance the stability of S3a; these are *extrinsic* as well as *kinetic stabilization* originating from high-affinity Ca^{2+}-binding. As shown by spectral analysis, S3a contains one high-affinity and one low-affinity Ca^{2+}-binding site per subunit. Unfolding in the absence and in the presence of Ca^{2+} gives evidence for extreme thermodynamic and kinetic stabilization of the protein: ΔG_{stab} is shifted from 81 ± 8 to 137 ± 11 kJ/mol(dimer), T_m from 53 to 69°C, and the half-time of unfolding from 8 min (in 2.5 *M* GdmCl) to > 9 h (in 7.5 *M* GdmCl) (Figure 9). The fact that the Ca^{2+} concentration in the spherules is sufficient for the complete complexation of the stress protein suggests that under condition of physiological stress the high expression of S3a provides *Physarum polycephalum* with an extremely potent compatible solute (Kretschmar et al., 1999b; Kretschmar and Jaenicke, 1999).

2. Protein S

The Ca^{2+}-binding two-domain crystallin homolog Protein S from

Myxococcus xanthus shares not only its topology with γB-crystallin, but also the difference in stability of its domains. The stability and Ca^{2+}-binding were monitored by spectral and calorimetric techniques (Wenk and Mayr, 1998; Wenk and Jaenicke, 1999). The combination of the two approaches allowed both the mechanism and the thermodynamics of unfolding/refolding to be analyzed. Regarding Ca^{2+}-binding and its extrinsic stabilizing effect, the monomeric two-domain PS follows the same pattern as the single-domain Spherulin 3a, except that the stoichiometry of Ca^{2+}-binding is still unclear: Equilibrium dialysis data point to two binding sites (K_D = 27 and 76 μ*M*) for the complete two-domain protein (Teintze et al., 1988), whereas X-ray crystallography gives the same result for the isolated N-terminal half-molecule (Wenk et al., 1999). With its γB-like topology, intact PS not only shows enhanced stability but also increased cooperativity of its equilibrium unfolding transitions, to the extent that, in the presence of Ca^{2+}, the bimodal profiles are transformed to a single sharp peak (Figure 10). The spectral changes clearly indicate that Ca^{2+} binding alters the tertiary structure of PS and its isolated domains, while the secondary structure of all three proteins remains practically uneffected; in terms of the overall structure, the Ca^{2+}-induced ~10% increase in sedimentation velocity suggests a compaction of the molecule to contribute to the extrinsic stabilization.

Chemical and thermal unfolding/refolding, both in the absence and in the presence of Ca^{2+}, are fully reversible. However, the calorimetric characteristics of the intact protein and its isolated domains PS-N and PS-C show significant differences. They refer to the denaturant concentrations required for 50% unfolding and to the cooperativity of the N → U transition. For the intact two-domain protein, independent folding/unfolding of the domains is observed only at low pH, when the urea-induced breakage of hydrogen bonds and charge repulsion (plus Ca^{2+} release) are superimposed. The same change in mechanism was found for the thermal transitions at 10 to 90°C; here, at pH 2 and 9 as well as in the absence of Ca^{2+}, two well-separated thermal transitions were observed, whereas at neutral pH the bimodal profile is not detectable. Considering the isolated domains, in the presence of Ca^{2+}, $\Delta G_{PS\text{-}N}$ exceeds $\Delta G_{PS\text{-}C}$; obviously, in the intact two-domain protein, the interactions between the domains result in an apparent destabilization of the N-domain with a concomitant increase in stability of the C-terminal half of the molecule (Figure 10). The thermal analysis of the monophasic profiles proves the separate domains to obey the two-state model; in contrast, intact PS can only be fitted assuming two transitions, the first attributable to the unfolding of the C-terminal half (including the loss of domain interactions) and the second to the unfolding of the N-terminal part. Comparing the calorimetric profiles of the isolated domains, similar values for the change in molar heat capacity (ΔC_p) and enthalpy (ΔH) are observed, as one would predict for proteins with similar size and fold (Myers et al., 1995). On the other hand, there is a striking difference of 20 degrees between the melting points of the two domains, reflecting the significantly higher thermodynamic stability of the N-terminal domain compared to its C-terminal counterpart (Figure 10, Table 5). In the case of the isolated domains,

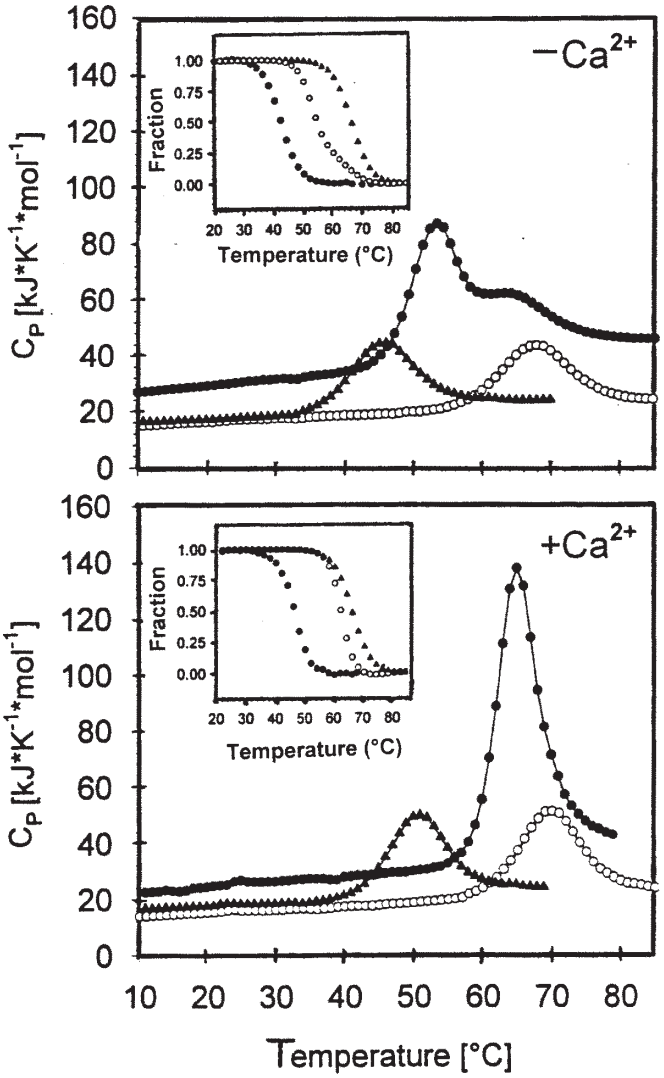

FIGURE 10. Comparison of DSC melting profiles of PS and its isolated domains in the absence and in the presence of Ca^{2+}. PS (●), PS-N (o), PS-C (▲) in 20 m*M* sodium cacodylate pH 7.0 *Upper frame:* in the presence of 1 m*M* EDTA; *lower frame:* in the presence of 3 m*M* $CaCl_2$. *Inserts:* Normalized temperature-induced unfolding transitions monitored by absorbance at 286 nm in the absence and in the presence of Ca^{2+} (Wenk, 1999; Wenk and Jaenicke, 1999).

the effects are similar but less pronounced; as has been mentioned, the intrinsic stability of the C-domain in intact PS exceeds the stability of PS-C, whereas for the N-domain the opposite holds true. Ca^{2+} binding, apart from enhancing both ΔG_{stab} and the cooperativity of unfolding, also strengthens the interactions between the separate domains such that a 1:1 mixture of PS-N and PS-C is able to form liganded "nicked protein S" (Wenk et al., 1999).

Considering the unfolding/refolding *kinetics* for the isolated domains, only monoexponential traces were obtained, as for other small all-β proteins (Capaldi and Radford, 1998). In the case of intact PS, only the unfolding can be fitted with one exponential, whereas refolding shows biphasic kinetics, indicating fold-

TABLE 5
Structure, Thermodynamics, and Kinetics of Protein S and its Separate Domains [a]

	PS	PS-N	PS-C
Residues	172 (A2-S173)[b]	88 (A2-V89)[b]	91 (M-Q90-S173+6H)[c]
Molecular mass (kDa)			
mass spectroscopy	18.661	9.384	10.249
analyt. ultracentrifuge[d]	19.6±1.2	9.5±0.2	10.2±0.3
$s_{20,w}$ (S) $- / + Ca^{2+}$	1.90 / 2.12	1.43 / 1.45	1.48 / 1.63
State of association	monomer	monomer	monomer
$c_{1/2,urea}$ (M) $- / + Ca^{2+}$		4.4 / 5.0	1.8 / 2.6
ΔG_{urea} (kJ/mol) $- / + Ca^{2+}$		21±2 / 31±3	15±2 / 20±2
T_m (°C) pH 2.0 $- / + Ca^{2+}$		52 / 52	30 / 30
pH 7.0 $- / + Ca^{2+}$	N[e]: 52 / 64	68 / 70	
	C[e]: 64 / 65		45 / 50

ing intermediates. Both the highly stable PS-N and its less stable counterpart PS-C unfold at the same rate ($k_{N \rightarrow U} \approx 9 \times 10^{-5}\ s^{-1}$), whereas for intact PS the unfolding rate of the cooperative unit of the interacting domains is slowed down 100-fold, suggesting that PS is stabilized kinetically due to a high activation energy barrier between the native and the unfolded states (Schindler et al., 1995; Wenk et al., 1998). In contrast to these results, in the structurally related γB-crystallin, the N-terminal domain is not affected in its stability, while the stability of the isolated C-domain is strongly decreased; hydrophobic domain interactions contribute to the intrinsic stability (Palme et al., 1997). In summary, Protein S exhibits a close similarity to other modular proteins that were previously shown to gain stability by mutual interactions of their domains to the extent that in some cases separate domains or truncated proteins were found to require their complementary parts for proper folding or assembly (Jaenicke, 1999). Considering the specific stabilization of the two microbial crystallin homologs by Ca^{2+}-ions, one wonders whether the extrinsic effects can be generalized; for βγ-crystallins the answer is negative, because neither γB nor βB2 exhibit Ca^{2+}-binding.

TABLE 5 (continued)

ΔG_{cal} (kJ/mol)	$-$ / + Ca^{2+}	N^e: 29 / 39	18 / 26	
		C^e: 16 / 25		16 / 20
$k_{N\rightarrow U}$ (s^{-1})	(pH 7.0 +Ca^{2+})	–	21	0.13
$k_{U\rightarrow N}$ (s^{-1})		9.0×10^{-7}	8.5×10^{-5}	9.6×10^{-5}

a 20 mM glycine/HCl pH 2.0, 20 mM sodium cacodylate pH 7.0, plus 1 mM EDTA or 3 mM $CaCl_2$, 20°C. $s_{20,w}$, sedimentation coefficient; $c_{1/2,urea}$, transition midpoint of urea denaturation monitored by absorption at 286 nm, fluorescence emission at 305 nm or CD at 222 nm. T_m and ΔG_{cal}, temperature and free energy of denaturation from calorimetry at 20-85°C (1 K/min). $k_{N\rightarrow U}$ and $k_{U\rightarrow N}$, microscopic rate constants of unfolding and folding in the absence of urea. $-$ / +Ca^{2+} refer to data in the absence and in the presence of 3 mM $CaCl^{2+}$. Data from Wenk & Jaenicke, 1999; Wenk et al., 1999.

b The N-terminal Met residues are cleaved off by *E. coli* methionyl aminopeptidase.

c To avoid degradation, recombinant PS-C was prepared with a His_6-tag.

d Results from sedimentation equilibria at 0.2-2.3 mg/ml initial concentration in the absence and in the presence of Ca^{2+} did not differ.

e For PS, N^e and C^e refer to the N- and C-terminal domain in the intact two-domain protein.

The N-terminal domain of βB2 provides an example of where higher-order interactions cause mutual stabilization of the protomer fold (Jaenicke, 1999). Pinpointing the structural basis for this lower stability is difficult, considering that pairwise comparisons of the various N- and C-terminal domains of β- and γ-crystallins show only around 30% sequence identity. However, in the native βB2-crystallin protein, the N-terminal domain is stabilized at the expense of a decrease in stability of the C-terminal one (Wieligmann et al., 1999). A contribution to this stability redistribution may reside in the asymmetric structural feature of the interface, namely, the covering of a surface hydrophobic patch on the N-terminal domain by a constrained sequence extension from the C-terminal domain (cf. Plate 4b). This mutual stabilization between nonidentical domains probably contributes to the observed heterologous

N:C domain pairing in native oligomeric β-crystallins as opposed to N:N and C:C pairings. The C-terminal domain only forms monomers in solution (Wieligmann et al., 1999), whereas the N-terminal domain provides a more favorable partner.

It is intriguing that at some stage during the evolution of the two-domain βB2-crystallin the N-terminal domain has effectively evolved a structural dependence on the C-terminal domain (Clout et al., 2000). Supposedly, the polypeptide is involved in domain swapping (Bax et al., 1990; Schlunegger et al., 1997); on the other hand, it has been invoked to have a role in solubilizing crystallin hetero-oligomers in the eye lens by subunit exchange (Slingsby and Bateman, 1990; Bateman and Slingsby, 1992). Both processes require the N-terminal domain to become unpaired from the C-terminal one. It may be assumed that both the solubilizing and the exchanging role of βB2-crystallin is aided by the ease of unfolding of the N-terminal domain.

IV. FUNCTION

It has been mentioned that proteins in general are multifunctional: they *fold* to *function in one or the other way* until they *undergo degradation* to serve as nutrients or to allow regeneration (Wetlaufer, 1980; Creighton, 1994). Thus, generally, evolution has selected proteins for characteristics at more than one level rather than solely for maximum stability. Crystallins give the impression of being exceptional, because they do not undergo any significant turnover in the eye lens; maintaining the refractive-index gradient as structural proteins seems to be their only function. This uniform role might therefore dictate adaptation for maximum stability, and yet crystallins are endowed with a range of stabilities. They are required, however, to interact with many different types of crystallins, both specifically (Slingsby et al., 1997) and nonspecifically (Tardieu and Delaye, 1988), dependent on spatial and species requirements, in other words, on context (de Jong et al., 1994; Nagl, 2001). Significantly, αB occurs in many other celltypes where it functions as a small heat shock protein (Jaenicke and Creighton, 1993; Ehrnsperger et al., 1998; Derham and Harding, 1999; Horwitz, 2000). In fact, the taxon-specific crystallins are classic examples of proteins that perform different functions depending on context (Wistow, 1993; Jaenicke, 1994); see Section IV.C.

A. Crystallins as Structural Proteins in Eye Lens Fiber Cells

1. Refractive and Light-Scattering Properties: Physical and Developmental Aspects

The visual function of the eye involves the lens as a focusing device that allows images to be formed on the retina. To serve this function, the eye lens has to fulfill two requirements, it has to provide transparency and a high refractive index, that is, low light scattering and high solubility of its constituent proteins. From the physical point of view, transparency is limited by absorption and light scattering of visible light. In the cataract-free lens, absorption in the visible wavelength range is negligible.

To understand how the cellular structure of the lens fulfills these biophysical requirements, it is necessary to describe its embryological development. Surface embryonic ectodermal cells invaginate to form the lens vesicle with cells on the retina side elongating to primary lens fiber cells filling the vesicle space. Cells on the cornea side remain a monolayer of epithelial cells, while those occupying the equatorial zone elongate to form secondary fiber cells that form a continuous layer overlaying the primary fibers (Bron et al., 2000). This process of secondary fiber formation continues throughout fetal and adult life, resulting in the mature lens being formed from numerous concentric shells, with the elongated fiber cells displaying hexagonal close packing. After gradually losing their intracellular organelles, the lens fiber cells retain exclusively the concentrated aqueous solution of the various eye-lens proteins. At this point, light scattering may originate from the differing refractive indices of the membrane and the cytoplasm of the fiber cells. The experimental evidence for this refractive index difference is clearly seen in the diffraction peaks recorded when laser light is passed through a thin peripheral section of the lens (Benedek et al., 1979). The absence of diffraction when light is directed along the optical axis is presumably a consequence of the continuous gradual change in orientation between layers of cells along this axis (like in many hard won protein crystals that do not refract X-rays?).

Although it is commonly referred to as a "crystalline lens", it was postulated on theoretical grounds that a liquid-like order was the basis of transparency of ocular tissues (Benedek, 1971). However, light scattering, due to the significant refractive index increment and the large molecular masses of eye lens proteins, is expected to interfere with transparency. Because during eye-lens development primary epithelial cells lose their nuclei and organelles, α-crystallins remain as the largest multimeric component in the highly concentrated reservoir of crystallin structural proteins in the fiber cells. Quantitative measurements over a wide range of protein concentrations showed that light scattering first exhibited the expected linear increase with concentration. However, beyond ~ 0.2 g ml^{-1}, a decrease was observed so that under physiological conditions the core of the lens exhibited practically unperturbed transparency (Figure 11). Analyzing the local organization of the solutions by X-ray scattering, it became clear that beyond a limiting protein concentration, the fluctuations of the refractive index are strongly affected by a short-range, liquid-like order of the scattering particles so that scattering is quenched to a high extent (Delaye and Tardieu, 1983; Tardieu and Delaye, 1988; Vérétout et al., 1989). Thus, both lens transparency and refraction derive from high protein concentrations.

The transmission of light along the optical axis of the lens involves protein components made throughout its development and growth. Differential gene activation of crystallin genes during development creates different levels of crystallin proteins along the optical axis (Piatigorsky and Zelenka, 1992). Proteins expressed early occupy the lens core region and have to last a lifetime because the cells lose their biosynthetic and degradative machinery. The design principle of vertebrate lenses thus is one of deposition of complex mixtures of crystallins that vary in their relative proportions along the optical axis, put in place by differential gene activation

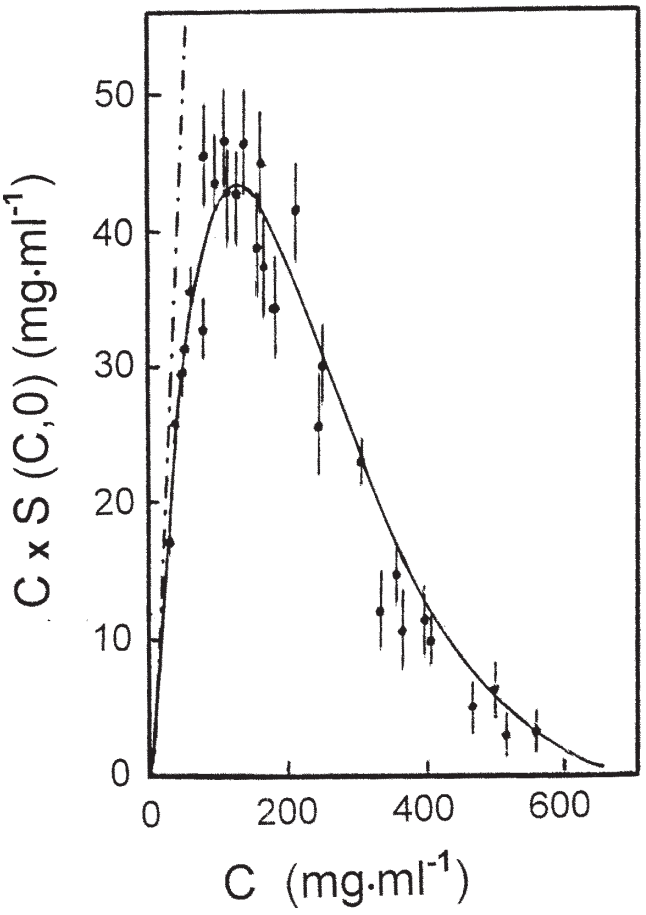

FIGURE 11. Light-scattering intensity as a function of protein concentration C in calf-lens cortical cytoplasmic extracts (cf. Delaye and Tardieu, 1983). The dashed line (· — · —) depicts the linear C-dependence expected from Rayleigh's equation for an ideal polymer solution (van Holde et al., 1998).

during the species' lifespan. The dioptric power of the lens is determined not only by the lens shape but also by its refractive index gradient that derives from the developmental pathway. A refractive index gradient both increases the overall power of the lens and reduces spherical aberration (Maxwell, 1854). The optical quality of animal lenses is excellent, cones are visible through the intact optics of animal and human eyes (Hughes, 1996), yet there is great variety in certain lens parameters. The human and the fish lens represent two extreme kinds of lens reflecting their different optical specializations. In most terrestrial animals, the air-cornea interface provides the bulk of refraction with the lens being used for fine focusing over a range of distances. In diurnal animals, this accommodation is commonly achieved by a soft lens moulding into different shapes (Koretz and Handelman, 1988); as an exception, nocturnal animals such as rodents have a very hard lens and cannot accommodate by changing the shape of the lens (N.H. Lubsen, personal communication). In aquatic animals the lens has to provide all the refraction, so fish lenses are spherical and have a very high refractive index at the center. The fish lens

can be readily dissected into two parts, a hard nearly incompressible core region and a soft cortex; in the case of a small fish from Lake Tanganyika, the core radius represents precisely two thirds of the whole lens radius in all sizes of fish (Fernald and Wright, 1983). The human lens thickness along the optical axis varies with age growing from 3.7 mm at age 20 to 4.2 mm at age 60, with the equatorial diameter remaining constant at 9 mm after age 30 (Smith et al., 1992). Although the distinction between core and cortex is much less marked in humans compared with fishes, a central core region can be discerned on fine dissection (~7 mm in equatorial diameter) that has a characteristic protein electrophoresis pattern different from the cortex (Garland et al., 1996).

The detail of refractive index gradients ($\Delta n/c$) (which has been in dispute even in the spherically symmetrical fish lens) has been resolved recently in favor of a complex continual decrease of refractive indices (n) from the center (1.54) to the surface (1.36) (Kröger et al., 1994). Refractive index gradients have been measured for a wide age range of bovine lenses; it is in place even in the early fetus, spanning from 1.38 at the edge to 1.45 in the center, and steepening to 1.47 in the center of the oldest lens (Pierscionek and Augusteyn, 1992). The shape of the very shallow refractive index gradient in the biconvex spheroid human lens is difficult to measure; it is almost constant with $n \sim 1.40$. The above ranges of refractive indices values stem from massive differences in protein concentration. For example, if $\Delta n/c = 0.20$ ml g^{-1} is taken for total crystallins (Pierscionek, 1997), then the protein concentration of the fish lens increases from 0.13 g ml^{-1} at the edge to 1.05 g ml^{-1} at the center, while the human lens has a protein concentration around 0.32 g ml^{-1}. These data clearly show that in order to fulfill their optical function during the whole lifespan, eye-lens proteins have to be first and foremost soluble: the highly concentrated protein solutions of the cortex eventually become the (sometimes glassy) core and their concentrated solutions have to last a lifetime. High solubility and high intrinsic stability are not necessarily compatible; on the contrary, highly stable proteins are often found to exhibit low solubility. However, the glass-like center of the fish lens is robust as regards transparency, as evidenced from inspection of a cooked fish-eye. By contrast, the transparency of a concentrated solution is sensitive both to dilution and to changes to the protein molecules that decrease solubility. This is why the human lens is prone to nuclear cataract in old age.

2. Intermolecular Interactions

The three-dimensional structure of proteins and their assembly to form complex cellular structures are determined by two classes of *non-covalent, " weak" interactions*: electrostatic and hydrophobic. The electrostatic interactions include ion pairs, hydrogen bonds, weakly polar interactions, and v. d. Waals forces. Hydrophobic interactions imply v. d. Waals forces and hydration effects of non-polar groups; due to the superposition of significant enthalpic and entropic increments, their temperature dependence is complex and their contribution to protein stability still the subject of controversy (Baldwin and Eisenberg, 1987; Privalov and Gill, 1988; Dill, 1990; Creighton, 1991; Franks, 1995; Makhatadze and Privalov, 1995; Pace et al., 1996; Thornton, 2001; Jaenicke and Böhm, 2001).

Attempts to analyze the molecular basis of the high stability and the anomalous scattering behavior of the eye lens in terms of the various types of weak interactions between the crystallin components are complicated by two fundamental problems: (1) the question of how the marginal Gibbs free energy of stabilization of a given protein or a set of proteins is accumulated from the massive contributions of attractive and repulsive potentials between several thousand atoms and (2) our lack of understanding of nonideality in concentrated macromolecular polyelectrolyte solutions (Eisenberg, 1976; Tardieu et al., 1999). Using multimeric α-crystallin as a model, effects of ionic strength suggested the importance of coulombic interactions. The mixture of crystallins in the cytoplasm of the lens was found to display overall repulsive interactions determined essentially by the dominating effect of α-crystallin (Vérétout et al., 1989). As a consequence, scattering particles in a concentrated solution tend to show an even distribution without periodical order that in turn reduces light scattering and accounts for high transparency. For β- and γ-crystallin, interactions under physiological conditions (pH 6.8, 17 to 150 m*M* KCl, 7 to 31°C) were found to differ: While interactions between β-crystallins are repulsive and independent of temperature, those between γ-crystallins are attractive, increasing with decreasing temperature. γ-Crystallins, in fact, tend to undergo phase separation at low temperature (Tardieu et al., 1992). As mentioned, the molecular explanation of these observations is hampered by the fact that presently the question of how excluded volume, compactness, preferential solvation, and charge or charge-distribution translate into a structural model for the short-range, liquid-like order of a multicomponent system such as the cytosol of fiber cells cannot be answered. Quoting the authors, we conclude that "transparency may be achieved in many ways by adequate combinations of molecular weight and compactness. The constraint for transparency might not be as severe as thought previously. Many different proteins might have done as well. So the question remains why the crystallins were selected through evolution. Part of the answer probably lies in their stability and/or in their ability to incorporate different (modified) subunits. The charge seems to play only an indirect role (e.g., in preventing aggregation), since at the ionic strength prevailing *in vivo* charges are almost completely screened. Oligomers are a good way in forming globular particles with evenly distributed charge density; their polydispersity may, in addition, help to avoid crystallization" (Tardieu and Vérétout, 1991). The expanding list of enzyme-crystallins gives evidence that different proteins have indeed done as well (see below). Their common denominator is the combination of high stability and solubility; among the two, the selection pressure to maintain high solubility is acute. Two types of human congenital cataracts have been shown to be caused by point mutations to surface residues of γ-crystallin that appear to reduce the protein solubility, in one case even causing crystallization (Héon et al., 1999; Kmoch et al., 2000). It is perhaps significant that both mutations affect surface arginines, a polyvalent residue.

A general view of *excluded-volume effects* ("macromolecular crowding") on reactions that lead either to protein assembly or aggregation has been given recently by Minton (2000a). Considering the vertebrate eye lens, his distinction between "background molecules"

that do not interact specifically with either the reactants or products of a particular reaction, and "test species" involved in specific reactions or interactions, is difficult because of the complexity of the multicomponent system and our ignorance with regard to "specific reactions" taking place in the cytoplasm of fiber cells. At the given high protein level, in which the different macromolecular species occupy a large fraction of the total volume of the solution, crowding may affect a wide variety of reactions: (1) folding and association of proteins (Jaenicke, 1996a, 1998), (2) binding of folding/unfolding intermediates to molecular chaperones, e.g., α-crystallin (Horwitz, 1992; Carver et al., 1994; Ehrnsperger et al., 1998; van den Berg et al., 1999, 2000; Berr et al., 2000), (3) reversible binding of folding intermediates to (non-chaperone) proteins, (4) as a consequence of (3), self-assembly of homo- or hetero-oligomers and multimers (Lindner and Ralston, 1995, 1997; Liu et al., 1996; Rivas et al., 1999), (5) irreversible aggregation of misfolded proteins to form large particles (Wilf et al., 1985; Jaenicke and Seckler, 1997; Lansbury, 1999; Dobson, 1999), and finally (6) assembly of proteins to membranes, for example, of fiber cells. Figure 12 gives a schematic view of the underlying mechanisms, with the partially (un)folded polypeptide chain (I) as the central reactant. In the various processes, interactions between background and test species may be individually weak. However, the cumulative effect on the "test reaction" may be large in a crowded environment, for the simple reason that steric repulsion by excluding volume reduces the configurational entropy. This increases the Gibbs free energy of the solution, and hence stabilizes the native structure of globular proteins relative to less compact nonnative structures, thus favoring the formation of native protein complexes (Tellam et al., 1983; Minton, 2000a,b). At the upper limit of solubility, where phase separation may take place, "overcrowding" may enhance aggregation reactions of nonnative proteins leading to increased light scattering. Whether entangling of polypeptide chains or covalent cross-linking (e.g., by disulfide bridges) is involved in stabilizing aggregates depends on the specific local points of attachment (de Gennes, 1979; Jaenicke and Seckler, 1997; Liu et al., 1996). Apart from thermodynamic stabilization, volume exclusion in crowded solutions may also reduce the rates of diffusion-controlled reactions as a consequence of decreased diffusional mobility of the reactants. On the other hand, the rates of $\Delta G^{\ddagger}$ -limited association reactions may be enhanced by crowding, depending on the excluded-volume properties of the transition-state (cf. Jacob, 2000; Bieri and Kiefhaber, 1999, 2000).

Considering the large number of components in the eye lens fiber cell, Figure 12 gives an oversimplified picture. It is unlikely that under a given set of conditions all the indicated reactions will be equally important or take place simultaneously. In any case, it is evident that we are far from a quantitative understanding of "nonideality". Following thermodynamic arguments and the statistical-thermodynamic models for the estimation of excluded volume effects, it appears that relatively small deviations from ideality at high dilution may become important under crowded *in vivo* conditions (Zimmerman and Minton, 1993; Dill and Stigter, 1995; Minton, 1998, 2000b; Ellis, 2001).

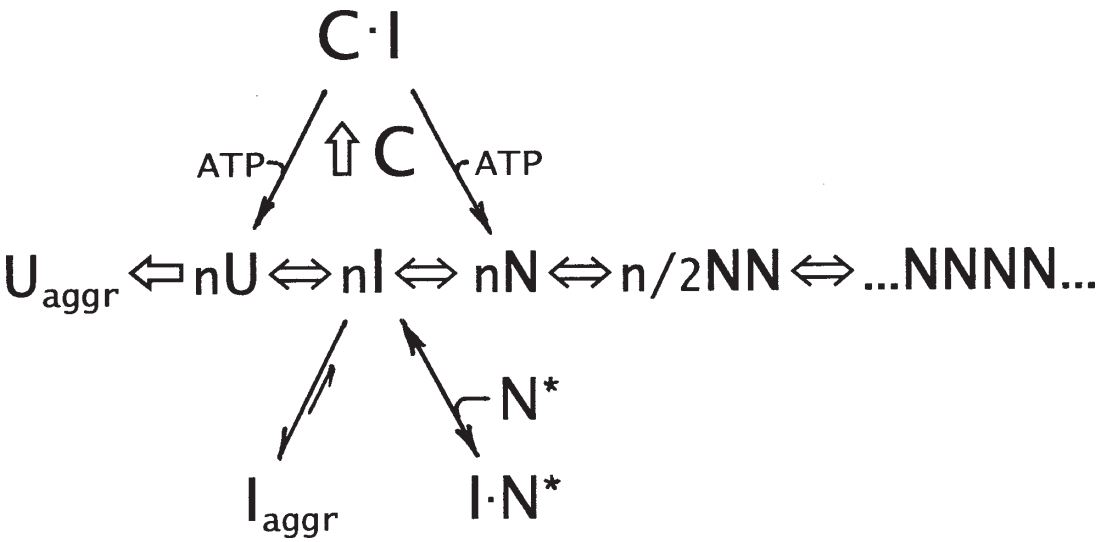

FIGURE 12. Reactions involved in the folding and association of proteins at high protein concentration. The simple variant of the three-state equation (Eq. 4): nU ⇔ n I ⇔ N_n with U = unfolded polypeptide, I = non-native (partially folded) intermediate and N = native protein, needs to be modified because of the kinetic partitioning of folding and aggregation (Jaenicke, 1996a; Jaenicke and Lilie, 2000) and molecular crowding (Minton, 2000a,b). Starting from the folding intermediate I, the horizontal sequence of reactions ends either in practically irreversible aggregation (U_{aggr}) or in assemblies of compact native subunits with well-defined quaternary structures (from dimers up to multimers …NNNN…) as final products. At high concentrations of other protein components (N*), side reactions may cause the formation of reversible intermediate complexes (I · N*) . Polymerization of the intermediate leads to large arrays of misfolded protein (I_{aggr}), ending up in amyloids etc. In the cell (as well as *in vitro*), molecular chaperones (C) may interfere with the latter process (Jaenicke, 1998).

According to the concept of *hydration forces*, the noncovalent polar interactions involved in highly concentrated polyelectrolyte solutions have been assumed to propagate over appreciable distances into the aqueous medium (Parsegian et al., 1986). The reason is that water molecules of hydration have been shown to exhibit a significant preferential orientation in the adjoining hydration sphere, or even in subsequent layers of water (Israelachvili, 1985; van Oss and Good, 1988). The underlying mechanism may be described by repulsive hydrogen bonding interactions between hydrophilic molecules or surfaces as hydrogen-acceptors, on the one hand, and water molecules of the aqueous medium on the other. With hydrophobic molecules or surfaces, these net hydrogen-bonding interactions tend to be attractive; commonly, they are considered as hydrophobic interactions (van Oss, 1993).

The physical state of the cytoplasmic protein solution within lens fiber cells depends critically on temperature, crystallin composition and a variety of other parameters and is prone to *phase separation* (Benedek, 1971). For example, lowering the temperature of a calf lens below 15°C leads to "cold cataract" as the result of a separation of the concentrated cytoplasmic protein solution into a coexisting protein-rich and a protein-poor phase. The complete segregation of protein and water is unfavorable for entropic reasons; thus, to an

extent determined by the temperature, the protein phase must contain water molecules and *vice versa*. The spatial fluctuation in the protein density from one phase to the other produces sufficient light scattering to cause opacification of the lens; after raising the temperature, the lens becomes clear again (Tanaka and Benedek, 1975). The actual temperature of phase separation (T_c) depends on the net attractive interprotein interaction energy; it rises as the interprotein interaction increases. If it increases above body temperature, the eye lens cytoplasm becomes opaque. Thus, the increase in light scattering accompanying the phase separation provides a means to quantify the net attraction within the multicomponent system of the eye lens. γ-Crystallins cluster into three groups characterized by increasing values of T_c: The lowest is mammalian γS, intermediary is typified by bovine γB and γD, and high T_c is typified by γE and γF (Siezen et al., 1988; Norledge et al, 1997b; cf. Table 1). The ratio of Arg/Lys is highest in the cryoproteins and lowest in γS-crystallin. The polyvalent guanidinium side chain allows ion-pair formation "in all directions". Indeed, in the 1.2 Å structure of γB, much of the protein-water structure exhibited a remarkably low level of conformational disorder, with arginine-containing ion pairs dominating the protein surface interactions (Kumaraswamy et al., 1996). At the side-chain level, arginines can more readily contribute toward a decrease in protein entropy than lysines that tend to "remain in solution". Presumably, this has some effect on the net attractive inter-protein interaction energy. Figure 13 shows the phase diagrams for the simple liquid-liquid phase separations in two binary aqueous protein solutions, illustrating the significant differences between two closely related proteins γD- and γE-crystallin (Benedek, 1997).

The overall distribution of the γ-crystallin family within a particular lens shows a correlation with phase separation behavior. γS-crystallin is located in the low refractive index outer regions of the lens as a result of synthesis after birth (Slingsby, 1985; Siezen et al., 1988). The high T_c proteins are synthesized early and therefore are enriched in the core region (de Jong et al., 1994). Low T_c γ-crystallins only phase-separate when solutions are extremely concentrated and they occupy an intermediary position along the refractive index gradient. The propensity of certain γ-crystallins to easily form a concentrated phase thus probably reflects their good packing properties. In the very high refractive index glass-like lenses, such as the core of the fish lens, γ-crystallins (but not γS) have numerous methionines on their domain surfaces (Slingsby et al., 1991) making them less polar than γ-crystallins from other species (Pan et al., 1995). We have argued that sulfur-arginine residues may assist in monomer-monomer interactions of the glass, much as these residues have been implicated in mediating subunit-subunit interactions in oligomers (Argos, 1988; Janin et al., 1988). Furthermore, the high polarizability of sulfur-containing residues may contribute directly to the high refractive index.

In order to get insight into *specific protein-protein interactions* between various crystallins at the atomic level, NMR spectroscopy has been shown to be a promising approach because signals assigned to flexible terminal extensions, such as the γ-crystallin C-terminal extension and the γS N-terminal extension (Cooper et al., 1994a), the

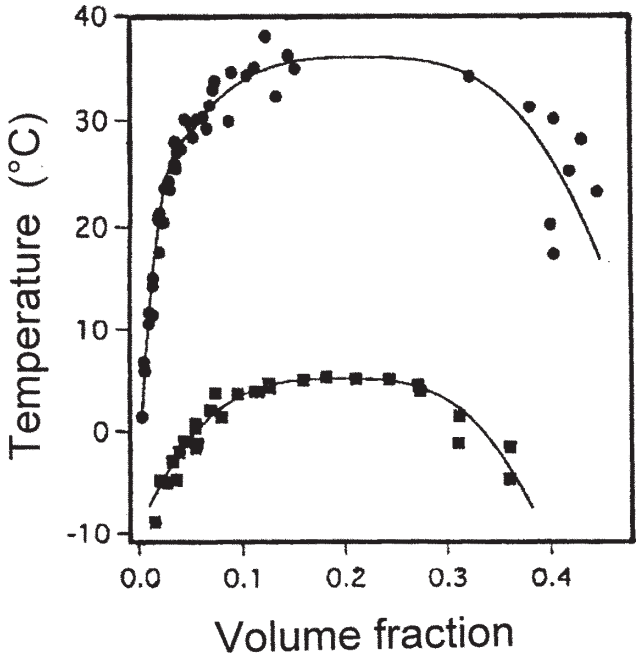

FIGURE 13. Coexistence curves for liquid-liquid phase separation in binary aqueous solutions of γD- (■) and γE-crystallin (•), measured at pH 7.1 in 100 m*M* phosphate buffer, ionic strength 240 m*M* (Broide et al., 1991; Benedek, 1997).

α-crystallin C-terminal extension (Carver et al., 1994) and the βB2-crystallin N- and C-terminal extensions (Carver et al., 1993a,b) allow protein-protein interactions in crystallin mixtures and nuclear or cortical lens homogenates to be compared (Cooper et al., 1994b). In both homogenates, resonances from the extensions were readily observed, suggesting that these regions are not involved in crystallin-crystallin interactions. In cortical homogenate, resonances from the short N-terminal extension of γS are also present. As taken from the relative intensities of the two homogenates, the cortex region exhibits significantly higher flexibility than the nuclear region. In both homogenates, the C-terminal extensions of βB2 and γB are not detectable; evidently, these regions are either in contact with each other, or they interact with other crystallins. Similar effects were obtained for mixtures of the individual crystallins. Taken together, the results are in accordance with the above mentioned short-range order of the crystallins within the lens.

3. Cataract

Cataract is a pathological opacity interfering with transparency that is often a consequence of wrong protein-protein interactions leading to the condensation of eye lens proteins into randomly distributed aggregates with average molecular masses beyond 50 MDa (Benedek, 1971, 1997). This definition correlates the physiological defect with the loss of solubility of specific proteins, thus indicating a mechanistic relationship between cataract formation and molecular diseases such as sickle-cell anemia, Alzheimer's disease and other amyloidoses. In the case of cataract, the wrong interactions are caused either by disturbances to the regular cytoplasma-membrane lattice repeat of the lens, or

by perturbations of the local short-range order of the crystallins in the interior of the fiber cells. From the physicochemical point of view, the spatial fluctuations of protein density responsible for lens opacification are attributable to either osmotic pressure effects, or to the spontaneous phase separation of the protein solution into coexisting protein-rich and protein-poor phases, or to the intrinsic instability of the cytoplasmic protein solution.

Osmotic cataract is attributable to the accumulation of water within the lens (Harding and Crabbe, 1984). Because of the high protein concentration in the cytoplasm of its fiber cells, the chemical potential for water in the lens interior is much lower than the water chemical potential in the aqueous environment of the lens. In order to avoid a flow of water into the lens, active pumps in the lens epithelial cells carefully compensate the gradient. If the pumps do not work for one reason or the other, there will be an influx of water into the lens. The decrease in overall protein concentration may result in impaired vision, for various reasons: (1) Refractive index changes affect focusing on the retina; (2) the accumulation of "water droplets" with dimensions exceeding the wavelength of light leads to lens opacification; (3) loss of integrity of membranes and gap junctions results in the partial destruction of the cellular compartmentalization, which may alter the subtle balance of phase equilibria in the multicomponent system of the cytoplasm by mixing up intracellular and extracellular components; (4) the dilution of protein concentration negates the effects of short-range order that reduces the normal light scattering of individual protein molecules. Some of these effects are reversible if the pump action can be restored before too much mechanical damage is done to the cell and cellular order.

Cataract that stems from *phase separation* can also be reversed if the proteins remain native and the parameters of the phase equilibria restored to normal. As γ-crystallins are thermodynamically stable, the small temperature changes that can cause cold cataract will have little effect on the conformation of individual protein molecules, rather they perturb the attractive interactions between properly folded molecules. However, dimerization, including cystine cross-linking, dramatically shifts T_c downward such that phase-separation can occur at body temperature, thus explaining the physical basis of a human juvenile hereditary cataract bearing a surface point mutation at Arg14Cys (Pande et al., 1995, 2000).

The aforementioned example highlights how a slight structural alteration can have a strong cataractogenic effect, derived in this case from a single point mutation in a rare hereditary disorder. Cataract, however, is mainly a problem of old-age with current levels of surgery remaining too low to tackle the backlog of cataract blind, estimated to be 16 to 20 million world-wide, and to stem the rising world incidence due to the ageing population. Major conformational changes in lens crystallins that occur as a function of age have many causes, and, like the cataracts they cause, are largely irreversible.

Conformational changes to crystallins can occur at any of the various levels of topology and hierarchy. They can originate from a variety of *covalent changes*: (1) Missense and nonsense (brutal change) mutations that usually cause congenital cataracts in children (Hejtmancik, 1998; Francis et al., 2000); (2) deamidation is

probably the smallest chemical change that befalls crystallins, but it does alter the charge balance. Deamidation of human γ-crystallins is correlated with aging (Hanson et al., 1998; Ma et a., 1998), and with increased insolubilization of crystallins, particularly γS (Hanson et al., 2000) for which site-specific deamidation has also been shown to be associated with cataract (Takemoto and Boyle, 2000); (3) oxidation of cysteine and methionine residues (Hanson et al., 2000); (4) peptide cleavage from proteolysis and free radical damage (Azuma et al., 1997; David et al., 1996; Lampi et al., 1998; Ma et al., 1998; Werten et al., 1999); (5) metabolite modification such as glycation (Harding and Crabbe, 1984) and UV irradiation (Truscott, 2000). On the other hand, purely *noncovalent conformational changes* can be endured by crystallins. The most susceptible crystallins are those of low stability that unfold in the presence of low denaturant concentrations, that is, mainly acidic βA3-crystallin (Werten et al., 1996), βB2-crystallin (Trinkl et al., 1994; Wieligmann, 2000), and α-crystallin (van den Oetelaar and Hoenders, 1989). As regards formation of light-scattering aggregates, evidently, βB2 can be thermally unfolded without aggregating (Horwitz et al., 1986; Maiti et al., 1988); similarly, heat-treated α-crystallin can endure massive loss of β-sheet (Surewicz and Oleson, 1995), but seems to neither dissociate nor aggregate (Carver et al., 1993a). The cataractogenic crystallins are thus more likely to be those that are the least stable, the least soluble, and the most prone to irreversible aggregation following unfolding at ambient temperature. Age-related cataract involves the superposition of the above-mentioned covalent modifications onto the age-related conformational effects. The structural consequences of these covalent or noncovalent structural changes will to some extent determine which of the various hierarchical levels is effected. Obviously, a point mutation or chemical modification that strikes a conserved structural feature of any of the βγ-crystallin double Greek-key domains, such as the folded β-hairpins, the tyrosine corner or the compact core, will have a major effect on the intrinsic stability of the protein. However, less serious changes at higher levels of organization, such as domain- or subunit-pairing, may also cause drastic changes of oligomer solubility and stability. In this regard it is noteworthy that βB2-crystallin is a promiscuous partner having solubilizing effects on other β-crystallin polypeptides (Bateman and Slingsby, 1992; Feng et al., 2000); thus, changes to it will have consequences not only for the β-crystallin heterodimers, but for the higher-order oligomers as well. The assembly of the highest-order β-crystallin (βH) is dependent on the full-length βB1-crystallin, which has an ~ 55 residue N-terminal extension. Progressive truncation of this extension with age causes the disassembly of βH-crystallin (David et al., 1996; Ajaz et al., 1997).

The consequence of these changes is that the more they destabilize the monomer or oligomer, the sooner they will be subjected onto the irreversible pathway of denaturation and consequent aggregation, unless rescued by binding to α-crystallin as a chaperone (Horwitz, 1992). Both αA- and αB-crystallin exhibit high chaperone efficiency, binding misfolded proteins with high affinity and stoichiometry but without substrate release (Lee et al., 1997; Ehrnsperger et al., 1998; Berr et al., 2000). In living cells the bound protein substrates are held until either directed to the proteoly-

sis machinery or passed onto ATP-dependent chaperones for refolding (Wickner et al., 1999). Neither of these options is available to the lens crystallins. There is some evidence that the conformational state of the substrate βγ-crystallins can be described as early unfolding intermediates on the irreversible pathway toward aggregation and precipitation (Das et al., 1999; Treweek et al., 2000). The burden of cataract prevention therefore will revolve on maintaining the short-range order of these complexes or increasing the thermodynamic and kinetic stability of the crystallins. There are several types of cataract, and for each of them not only the physical parameters and the chemical composition of the cytoplasm are important, but also the spatial distribution of the various protein components (Duncan, 1986; Nugent and Whelan, 1984; Tardieu and Delaye, 1988; Slingsby and Clout, 1999; Podos and Yanoff, 1992; Benedek, 1997).

B. Microbial Crystallins

The common denominator of eye-lens γ-crystallins and their structural homologs in microoganisms is their high intrinsic stability, especially in a dehydrated environment. From the functional point of view, the microbial crystallins differ widely. For one of them, spherulin 3a from *Physarum polycephalum*, still no clear-cut explanation can be given for its high expression under various stress conditions. During its life cycle, the polynuclear plasmodia of the slime mold in its diplophase undergo a light-induced shift to form sporangia and, after meiosis, haploid spores. After germination, these differentiate into two mating types whose zygotes close the cycle by "mitosis without cell division", thus ending up with plasmodia again. Under unfavorable growth conditions, cell differentiation leads to microplasmodia and finally to macrocysts, *spherules*, the stress-resistant durable form of the organism (Jump, 1954). "Spherulation" is accompanied by the synthesis of a variety of mRNAs coding for the structural proteins S1a/S1b, S2a, S3a, and a set of homologous 28 to 36 kDa cell-wall glycoproteins. S3a is highly soluble due to its high content of polar residues and contains neither a signal sequence nor sequons for glycosylation. These properties suggest either a function as a long-term nutrient pool or as a water-binding cytosolic storage protein. The latter function is in accordance with the observation that spherules can be readily activated just by rehydration to form plasmodia again (Sauer, 1986; Bernier et al., 1987). As has been shown (cf. Section III.D.1), S3a is dramatically stabilized by Ca^{2+}-ions under conditions present in the macrocysts. Obviously, under physiological stress, especially after desiccation, spherulin 3a is accumulated as a compatible solute, thus allowing the macrocysts during dormancy to reversibly trap water in their cytoplasm (Kretschmar et al., 1999b).

Myxococcal Protein S is the main component constituting the outer coat of the stress-induced *myxospores* of the Gram-positive soil bacterium *Myxococcus xanthus*. In the complex life cycle of the organism, nutrient, or water deficiency cause cell aggregation followed by formation of fruiting bodies and finally myxospores. The latter are the cryptobiotic form preserving viability of the bacterium over long periods of dehydration, temperature extremes, and even UV radiation. After fruiting-body formation, the level of PS reaches 15% of the total

cytoplasmic protein of the vegetative cells. The release of the protein by the lysis of about 80% of the cells allows the Ca^{2+}-dependent coating of the residual 20% with a multilayer assembly of Protein S. In the interior of the spores, only traces of PS are detectable. Evidently, the protein has a protective function that is brought to an end by solubilizing the surface layer in the presence of aqueous salt solutions or chelators with high Ca^{2+}-affinity (Wireman and Dworkin, 1977; Inouye et al., 1979a,b, 1981; Inouye and Inouye, 1987; Teintze et al., 1991).

In the case of the yeast-killer toxin WmKT from *Williopsis mrakii* and the proteinase inhibitor SMPI from *Streptococcus nigrescens* the respective functions are obvious. The first is a 9.5-kDa toxin that is secreted into the growth medium by certain yeasts to inhibit the simultaneous growth of competing strains; the target is the cell wall of the competitors, the mechanism: blocking β-glucan synthesis (Yamamoto et al., 1986). The second is a 102 residues, one-domain metallo-proteinase inhibitor that gains its intrinsic stability mainly from its Greek-key topology; two disulfide bonds are of lesser importance (Ohno et al., 1998). As its sequence homology to eye-lens crystallins is negligible, SMPI may be considered an example of convergent evolution. Both proteins, WmKT and SMPI, share their high intrinsic stability at extremes of pH and temperature with other enzyme inhibitors, evidently an important property for proteins secreted into the external medium.

C. Enzyme Crystallins with and without Catalytic Activity

As has been mentioned, focusing of light requires a lens to have a higher refractive index than the surrounding medium. In the eye lens, this is brought about by high concentrations of proteins, mainly αβγ-crystallins. The fact that the refractive-index increment of proteins does not vary over a wide range indicates that any protein could serve as "crystallin" (cf. Section IV.A.2). Actually, some of the most highly expressed eye-lens proteins are not the common *ubiquitous αβγ-crystallins*, but *taxon-specific enzyme-crystallins*. In the lens of some species, they amount to a minimum of 10% of the total protein, often they reach much higher levels. Table 6 summarizes a number of examples from different evolutionary lineages. Some of them represent central metabolic enzymes occurring in body cells and in the eye lens, and *sharing* one and the same gene (Wistow, 1993, 1995; Piatigorsky and Wistow, 1989, 1991; Piatigorsky and Zelenka, 1992). During evolution they must have switched directly to their new role as structural eye-lens proteins by modification of gene expression without prior gene duplication. This kind of *gene recruitment* reverses the conventional view that gene duplication must precede the acquisition of new protein functions (Wistow and Piatigorsky, 1987, 1988). Other examples illustrate the alternative, whereby recruitment followed gene duplication and divergence and hence can be accompanied by loss of catalytic function. This supports the conclusion that taxon-specific enzyme crystallins were not recruited for metabolic or catalytic reasons; instead, their abundance argues that they serve mainly as structural proteins contributing merely to the refractive-index and/or to the solubility properties in the complex multicomponent system of the lens. Thermodynamic (and kinetic) stability is another important property of eye-lens proteins. Therefore, it is possible that during evo-

TABLE 6
Taxon-Specific Enzyme Crystallins and Their Relationships with Enzymes[a]

Crystallin	Distribution	Identical with (=), or related to (~) [b]
δ	most birds, reptiles	= argininosuccinate lyase
ε	some birds, crocodiles	= lactate dehydrogenase (LDH-M_4)
ζ	guinee pig, camel, llama	= NADPH:quinone oxidoreductase
η	elephant shrew	= aldehyde dehydrogenase 1
ι	gekko (*Lygodactulus pictatus*)	= retinol-binding protein (type 1)
λ	rabbit, hare	~ hydroxyacyl CoA dehydrogenase
μ	kangaroo, quoll	~ ornithine cyclodeaminase
π	gekko (*Phelsuma serraticauda*)	= glyceraldehyde-3P dehydrogenase
ρ	frogs, gekko (*Lepidodact. lugubris*)	~ NADPH-dependent aldose reductase
σ	cephalopods	~ glutathione S-transferase
τ	many vertebrates	~ α-enolase
ω/Ω	octopus and squid	~ aldehyde dehydrogenase 1/2

a Examples taken from Piatigorsky & Wistow, 1989; Wistow, 1993, 1995; Jimenez-Asensio, 1995; Werten et al., 2000; van Boekel et al., 2001.

b = Refers to identical genes ; ~ symbolizes relationships based on sequence homologies or topological similarities.

lution proteins were recruited simply because of their high intrinsic stability. Keeping multifunctionality in mind, evidently, subsidiary roles such as sequestering NAD(P)H to protect the lens against oxidation or damage from UV radiation, are conceivable (Wistow et al., 1987; Wistow and Piatigorsky, 1987; Piatigorsky and Wistow, 1989, 1991; Jimenez-Asensio et al., 1995; Werten et al., 2000; Berr et al., 2000; van Boekel et al., 2001). The specific requirement in sharing or recruiting of a gene is that during evolution its different functions may be exposed to widely differing selective constraints so that adaptive changes favorable for one function may be deleterious for another. Conflicts like that may be resolved either by reversing the recruitment or by gene duplication; both strategies have been observed for enzyme crystallins.

V. CONCLUSIONS

The eye and its architecture, at the macroscopic, microscopic and molecular level, is a "joy forever". Artists, poets, and naturalists are equally attracted by its properties (Huxley, 1990; Darwin, 1859). The principle focus of the present review is on the eye lens. We covered some of the variety associated with the structure-function relationship of its building blocks, certain cell-biological and genetic aspects involved in its phylogenetic and ontological development, and some of the problems when its structure is destabilized. An enormous amount of knowledge has been accumulated, motivated mainly by the pathology of the eye lens, cataract, which is widespread, and therefore of enormous medical (and economical) relevance world-wide. The complexity of the system does not allow easy answers in connection with either its origin or its treatment. By emphasizing the current state of knowledge on the thermodynamic and kinetic basis of crystallin stability, and placing this in the context of a much wider body of information on protein stability we hope that some clarity has been achieved.

ACKNOWLEDGMENTS

We would like to thank our coworkers quoted in the references for their enthusiasm and Dr. Franz X. Schmid for critical comments. Fruitful discussions with Drs. Rudi Glockshuber, Nicolette H. Lubsen, Annette Tardieu, Graeme Wistow, and the members of the Human Capital and Mobility and the Biomed Programs of the European Community are gratefully acknowledged. Work performed in our laboratories was generously supported by the two research programs of the European Community as well as the Deutsche Forschungsgemeinschaft (DFG Grant Ja 78/32), the Fonds der Chemischen Industrie, the Fogarty International Center at the National Institutes of Health, Bethesda, MD (USA), the Max Planck Gesellschaft, and the Medical Research Council (London).

REFERENCES

Abgar, S., Backmann, J., Aerts, T., Vanhoudt, J., and Clauwaert, J. (2000) *Eur. J. Biochem.* **267**, 5916–5925.

Ajaz, M.S., Ma, Z., Smith, D.L., and Smith, J.B. (1997) *J. Biol. Chem.* **272**, 11250–11255.

Ansari, A., Jones, C.M., Henry, E., Hofrichter, J., and Eaton, W.A. (1992) *Science* **256**, 1796–1798.

Antuch, W., Günthert, P., and Wüthrich, K. (1996) *Nature Struct. Biol.* **3**, 662–664.

Argos, P. (1988) *Protein Eng.* 2, 101–113.

Auerbach, G., Ostendorp, R., Prade, L., Korndörfer, I., Dams, T., Huber, R., and Jaenicke, R. (1998) *Structure* **6**, 769–781.

Azuma, M., Fukiage, C., David, L.L, and Shearer, T.R. (1997) *Exp. Eye Res.* **64**, 529–538.

Bagby, S., Harvey, T.S., Eagle, S.G., Inouye, S., and Ikura, M. (1994a) *Proc. Natl. Acad. Sci. USA* **91**, 4308–4312.

Bagby, S., Harvey, T.S., Eagle, S.G., Inouye, S., and Ikura, M. (1994b) *Structure* **2**, 107–122.

Bagby, S., Harvey, T.S., Lewis, E.K., Eagle, S.G., Inouye, S., and Ikura, M. (1994c) *Biochemistry* **33**, 2409–2421.

Bagby, S., Go, S., Inouye, S., Ikura, M., and Chakrabartty, A. (1998) *J. Mol. Biol.* **276**, 669–681.

Baldwin, R.L. and Eisenberg, D. (1987) Protein stability. In: *Protein Engineering* (Oxender, D.L. and Fox, C.F., Eds.) A.R. Liss, Inc. New York, 127–148.

Basak, A.K., Kroone, R.C., Lubsen, N.H., Naylor, C.E., Jaenicke, R., and Slingsby, C. (1998) *Prot. Eng.* **11**, 337–344.

Bateman, O. A. and Slingsby, C. (1992). *Exp. Eye Res.* **55**, 127–133.

Bax, B., Lapatto, R., Nalini, V., Driessen, H., Lindley, P.F., Mahadevan, D., Blundell, T.L., and Slingsby, C. (1990) *Nature* **347**, 776–780.

Beissinger, M. and Buchner, J. (1998) *Biol. Chem.* **379**, 245–259.

Beissinger, M., Rutkat, K., and Buchner, J. (1999) *J. Mol. Biol.* **289**, 1075–1092.

Benedek, G.B. (1971) *Appl. Opt.* **10**, 459–473.

Benedek, K. (1979). Phil. *Trans. R. Soc. London Ser. A,* **293**, 329–340.

Benedek, G.B. (1997) *Investigative Ophthalmology and Visual Science* **38**, 1911–1921.

Bennett, M.J., Choe, S., and Eisenberg, D. (1994) *Proc. Natl. Acad. Sci. USA* **91**, 3127–3131.

Bennett, M.J., Schlunegger, M.P., and Eisenberg, D. (1995) *Protein Sci.* **4**, 2455–2468.

Berbers, G. A. M., Hoekman, W. A., Bloemendal, H., de Jong, W. W., Kleinschmidt, T., and Braunitzer, G. (1984) *Eur. J. Biochem.* **139**, 467–479.

Berbers, G.A.M., Boermann, O.C., Bloemendal, H., and de Jong, W.W. (1982) *Eur. J. Biochem.* **128**, 495–502.

Bernier, F., Lemieux, G., and Pallotta, D. (1987) *Gene* **59**, 265–277.

Berr, K., Wassenberg, D., Lilie, H., Behlke, J., and Jaenicke, R. (2000) *Eur. J. Biochem.,* **267**, 5413–5420.

Bieri, O. and Kiefhaber, T. (1999) *Biol. Chem.* **380**, 923–929.

Bieri, O. and Kiefhaber, T. (2000) In: *Mechanisms of Protein Folding* (Frontiers in Molecular Biology, Pain, R.H., Ed.), Oxford University Press, Oxford, 34–64

Bieri, O., Wirz, J., Hellrung, B., Schutkowski, M., Drewello, M., and Kiefhaber, T. (1999) *Proc. Natl. Acad. Sci. USA* **96**, 9597–9601.

Bindels, J.G., Koppers, A., and Hoenders, H.J. (1981) *Exp. Eye Res.* **33**, 333–343.

Bindels, J.G., Bessems, G.J., de Man, B.M., and Hoenders, H.J. (1983a) *Comp. Biochem. Physiol. B.* **76**, 47–55.

Bindels, J.G., Bours, J., and Hoenders, H.J. (1983b) *Mech. Ageing Dev.* **21**, 1–13.

Bloemendal, H. and de Jong, W.W. (1991) *Progr. Nucleic Acid Res. Mol. Biol.* **41**, 259–281.

Blundell, T.L., Lindley, P., Miller, L., Moss, D., Slingsby, C., Tickle, I., Turnell, B., and Wistow, G. (1981) *Nature* **289**, 771–777.

Blundell, T.L., Lindley, P.F., Miller, L.R., Moss, D.S., Slingsby, C., Turnell, W.G., and Wistow, G.J. (1983) *Lens Res.* **1**, 109–131.

Böhm, G. and Jaenicke, R. (1994) *Int. J. Pept. Prot. Res.* **43**, 97–106.

Bova, M.P., Ding, L.L., Horwitz, J., and Fung, B.K.-K. (1997) *J. Biol. Chem.* **272**, 29511–29517.

Branden, C. and Tooze, J. (1998) *Introduction to Protein Structure* (2nd ed.) Garland Publ., New York, 27.

Broide, M.L., Berland, C.R., Pande, J., Ogun, O., and Benedek, G.B. (1991) *Proc. Natl. Acad. Sci. USA* **88**, 5660–5664.

Bron, A.J., Vrensen, G.F.J.M, Koretz, J., Maraini, G., and Harding, J.J. (2000) *Ophthalmologica* **214**, 86–104.

Capaldi, A.P. and Radford, S.E. (1998) *Curr. Opin. Struct. Biol.* **8**, 86–92.

Carpenter, J.F., Clegg, J.S., Crowe, J.H., and Somero, G.N. (Eds.) (1993) Compatible solutes and macromolecular stability. *Cryobiology* **30**, 201–241.

Carver, J.A., Aquilina, J.A., and Truscott, R.J.W. (1993a) B*iochim. Biophys. Acta* **1164**, 22–28.

Carver, J.A., Cooper, P.G., and Truscott, R.J.W. (1993b) *Eur. J. Biochem.* **213**, 313–320.

Carver, J.A., Aquilina, J.A., Cooper, P.G., Williams, G.A., and Truscott, R.J.W. (1994) *Biochim. Biophys. Acta* **1204**, 195–206.

Cavagnero, S., Debe, D.A., Zhou, Z.H., Adams, M.W.W., and Chan, S.I (1998) *Biochemistry* **37**, 3369–3376.

Clark, J.I. and Muchowski, P.J. (2000) *Curr. Opin. Struct. Biol.* **10**, 52–59.

Clout, N.J., Slingsby, C., and Wistow, G.J. (1997) *Nature Struct. Biol.* **4**, 685.

Clout, N.J., Basak, A., Wieligmann, K., Bateman, O.A., Jaenicke, R., and Slingsby, C. (2000) *J. Mol. Biol.* **304**, 253–257.

Clout, N.J., Kretschmar, M., Jaenicke, R., and Slingsby, C. (2001) *Struct. Fold. Design*, 9, 115–124.

Cooper, A. (2000) *Biophys. Chem.* **85**, 25–39.

Cooper, P.G., Carver, J.A., and Truscott, R.J.W. (1993) *Eur. J. Biochem.* **213**, 321–328.

Cooper, P.G., Carver, J.A., Aquilina, J.A., Ralston, G.B., and Truscott, R.J. (1994a) *Exp. Eye Res.* **59**, 211–220.

Cooper, P.G., Aquilina, J.A., Truscott, R.J.W., and Carver, J.A. (1994b) *Exp. Eye Res.* **59**, 607–616.

Creighton, T.E. (1991) *Curr. Opin. Struct. Biol.* **1**, 5–16.

Creighton, T.E. (1994) *Proteins: Structures and Molecular Properties*. W.H. Freeman, New York.

Dams, T. and Jaenicke, R. (1999) *Biochemistry* **38**, 9169–9178.

Dams, T., Auerbach, G., Bader, G., Jacob, U., Ploom, T., Huber, R., and Jaenicke, R. (2000) *J. Mol. Biol.* **297**, 659–672.

Darwin, C. (1859) *The Origin of Species by Means of Natural Selection*. J. Murray, London.

Das, K.P., Choo-Smith, L-P., Petrash, J.M., and Surewicz, W.K. (1999) *J. Biol. Chem.* **274**, 33209–33212.

Datta, S.A. and Rao, C.M. (2000) *J. Biol. Chem.* **275**, 41004–41010.

David, L.L., Lampi, K.J., Lund, A.L., and Smith, J.B. (1996) *J. Biol. Chem.* **271**, 4273–4279.

de Gennes, P.-G. (1979) *Scaling Concepts in Polymer Physics*. Cornell University Press, New York.

de Jong, W.W., Lubsen, N.H., and Kraft, H.J. (1994) *Progr. Ret. Eye Res.* **54**, 391–442.

de Jong, W.W., Caspers, G.-J., and Leunissen, J.A.M. (1998) *Int. J. Biol. Macromol.* **22**, 151–162.

Delaye, M. and Tardieu, A. (1983) *Nature* **302**, 415–417.

Derham, B.K. and Harding, J.J. (1999) *Progr. Ret. Eye Res.* **18**, 463–509.

Dill, K.A. (1990) *Biochemistry* **29**, 7133–7155.

Dill, K.A. and Stigter, D. (1995) *Adv. Protein Chem.* **46**, 59–104.

Dobson, C.M. (1999) *Trends Biochem. Sci.* **24**, 329–332.

Doty, P. and Myers, G. (1953) *Discuss. Faraday Soc.* **13**, 51–58.

Dove, W.F. and Rusch, H.P. (Eds.) (1980) *Growth and Differentiation in Physarum polycephalum*. Princeton University Press, Princeton, NJ.

Durchschlag, H. (1986) In: *Thermodynamic Data for Biochemistry and Biotechnology* (Hinz, H.-J., Ed.) Springer Verlag, Berlin, pp. 45–128.

Durchschlag, H., Zipper, P., Wilfing, R., and Purr, G. (1991) *J. Appl. Cryst.* **24**, 822–831.

Ehrnsperger, M., Buchner, J. and Gaestel, M. (1998) In: *Molecular Chaperones in the Life Cycle of Proteins: Structure, Function, and Mode of Action* (A.L. Fink and Y. Goto, Eds.) Marcel Dekker, New York, pp. 533–575.

Eisenberg, H. (1976) *Biological Macromolecules and Polyelectrolytes in Solution*. Clarendon Press, Oxford.

Ellis, R.J. (2001) *Curr. Opin. Struct. Biol.* **11**, 114–119.

Feng J., Smith, D.L., and Smith, J.B. (2000) *J. Mol. Biol.* **275**, 11585–11590.

Francis, P.J., Berry, V., Bhattacharya, S.S., and Moore, A.T. (2000) *J. Med. Genetics* **37**, 481–488.

Franks, F. (1995) *Adv. Protein Chem.* **46**, 105–139.

Franks, F., Mathias, S.F., and Hatley, R.H.M. (1990) *Phil. Toy. Soc. Lond. Ser. B* **326**, 517–533.

Ganea, E. and Harding, J.J. (2000) *Biochem. J.* **345**, 467–472.

Garland, D.L., Duglas-Tabor, Y., Jimenez-Asensio, J., Datiles, M.B., and Magno, B. (1996) *Exp. Eye Res.* **62**, 285–291.

Gloss, L.M. and Matthews, C.R. (1997) *Biochemistry* **36**, 5612–5623.

Goldberg, M.E., Rudolph, R., and Jaenicke, R. (1991) *Biochemistry* **30**, 2790–2797.

Grättinger, M., Dankesreiter, A., Schurig, H., and Jaenicke, R. (1998) *J. Mol. Biol.* **280**, 525–533.

Grainger, R.M. (1992) *Trends Genet.* **8**, 349–355.

Groenen, P.J.T.A., Merck, K.B., de Jong, W.W., and Bloemendal, H. (1982) *Eur. J. Biochem.* **225**, 1–19.

Groenen, P.J.T.A., Merck, K.B., de Jong, WW., and Bloemendal, H. (1994) *Eur. J. Biochem.* **225**, 1–19.

Groß, M. and Jaenicke, R. (1994) *Eur. J. Biochem.* **221**, 617–630

Haley, D.A., Horwitz, J., and Stewart, P.L. (1998) *J. Mol. Biol.* **277**, 27–35.

Hanson, S.R.A., Smith, D.L., and Smith J.B. (1998) *Exp. Eye Res.* **67**, 301–312.

Hanson, S.R.A., Hasan, A., Smith, D.L., and Smith, J.B. (2000) *Exp. Eye Res.* **71**, 195–207.

Harding, J.J. and Crabbe, M.J.C. (1984) In: *The Eye* (H. Dawson, Ed.), Vol. 1B, Academic Press, London, 207–492.

Hay, R.E., Andley, U.P., and Petrash, J.M. (1994) *Eye Res.* **58**, 573–584.

Hejtmancik, J.F. (1998) *Am. J. Hum. Genetics* **62**, 520–525.

Hemmingsen, J.M., Gernert, K.M., Richardson, J.S., and Richardson, D.C. (1994) *Protein Sci.* **3**, 1927–1937.

Héon, E., Priston, M., Schorderet, D.F., Billingsley, G.D., Girard, P.O., Lubsen, N., and Munier, F.L. (1999) *Am. J. Hum. Genet.* **65**, 1261–1267.

Horwitz, J. (1992) *Proc. Natl. Acad. Sci. USA* **89**, 10449–10453.

Horwitz, J. (2000) *Seminars Cell Dev. Biol.* **11**, 53–60.

Horwitz, J., McFall-Nagai, M., Ding, L-L., and Yaron, O. (1986). In: *Top. Ageing Res. Europe,* Vol.16, (Duncan, G., Ed.). EURAGE Rijkwijk, 227–240.

Horwitz, J., Huang, Q.-L., Ding, L., and Bova, M.P. (1998) *Meth. Enzymol.* **290**, 365–383.

Horwitz, J., Bova, M.P., Ding, L.L., Haley, D.A., and Stewart, P.L. (1999) *Eye* **13**, 403–408.

Huber, R. (1988) *Angew. Chem. Int. Ed. Engl.* **27**, 79–88.

Hughes, A. (1996) *Nature*, **380** 393–394.

Huxley, F. (1990) *The Eye: The Seer and the Seen.* Thames and Hudson, London.

Ingolia,T.D. and Craig, E.A. (1982) *Proc. Natl. Acad. Sci. USA* **79**, 2360–2364.

Inouye, M. and Inouye, S. (1987) *Meth. Enzymol.* **139**, 380–390.

Inouye, M., Inouye, S., and Zusman, D.R. (1979a) *Develop. Biol.* **68**, 579–591.

Inouye, M., Inouye, S., and Zusman, D.R. (1979b) *Proc. Natl. Acad. Sci. USA* **76**, 209–213.

Israelachvili, J.N. (1985) *Intermolecular and Surface Forces.* Academic Press, London.

Jacob, M., Schindler, T., Balbach, J., and Schmid, F.X. (1997) *Proc. Natl. Acad. Sci. USA* **94**, 5622–5627.

Jacob, M. (2000) *PhD Thesis*, University of Bayreuth.

Jaenicke, R. (1987) *Progr. Biophys. Mol. Biol.* **41**, 127–237.

Jaenicke, R. (1990) *Phil. Trans. Roy. Soc. London Ser.* **B326**, 535–553.

Jaenicke, R. (1991) *Eur. J. Biochem.* **202**, 715–728.

Jaenicke, R. (1994) *Naturwissenschaften* **81**, 423–429.

Jaenicke, R. (1996a) *Curr. Topics Cellular Regulation* **34**, 209–314.

Jaenicke, R. (1996b) *FASEB J.* **10**, 84–92.

Jaenicke, R. (1998) *Biol. Chem.* **379**, 237–243.

Jaenicke, R. (1999) *Progr. Biophys. Mol. Biol.* **71**, 155–241.

Jaenicke, R. (2000) *J. Biotechnology* **79**, 193–203.

Jaenicke, R. and Böhm, G. (1998) *Curr. Opin. Struct. Biol.* **8**, 738–748.

Jaenicke, R. and Böhm, G. (2001) *Meth. Enzymol.*, **334**, 438–469..

Jaenicke, R. and Creighton, T.E. (1993) *Current Biology* **3**, 234–235.

Jaenicke, R. and Lauffer, M.A. (1969) *Biochemistry* **8**, 3083–3092.

Jaenicke, R. and Seckler, R. (1997) *Adv. Protein Chem.* **50**, 1–59.

Jaenicke, R., Schurig, H., Beaucamp, N., and Ostendorp, R. (1996) *Adv. Protein Chem.* **48**, 181–269.

Janin, J. (1995) *Proteins, Struct. Funct. Genet.* **21**, 30–39.

Janin, J., Miller, S., and Chothia, C. (1988) *J. Mol. Biol.* **204**, 155–164.

Jedziniak, J.A., Kinoshita, J.H. Yates, E.M. Hocker, L.O., and Benedek, G.B. (1973) *Exp. Eye Res.* **15**, 185–192.

Jencks, W.P. (1969) *Catalysis in Chemistry and Enzymology*. McGraw-Hill, New York.

Jimenez-Asensio, J., Gonzalez, P., Zigler J.S., Jr., and Garland, D.L. (1995) *Biochem. Biophys. Res. Commun.* **209**, 796–802.

Jump, J.A. (1954) *Amer. J. Bot.* **41**, 561–567.

Kaiser, D., Maniol, C.C., and Dworkin, M. (1979) *Annu. Rew. Microbiol.* **33**, 595–639.

Kauzmann, W. (1959) *Adv. Protein Chem.* **14**, 1–63.

Kern, G. (1992) *Ph.D. Thesis*, University of Regensburg.

Kim, K.K., Kim, R., and Kim, S.-H. (1998) *Nature* **394**, 595–599.

Kirby, A.J. (1980) *Adv. Phys. Org. Chem.* **17**, 183–278.

Kmoch, S., Brynda J., Asfaw, B., Bezouska, K., Novák, P., Rezácová, P., Ondrová, L., Filipec, M., Sedlácek, J., and Elleder, M. (2000) *Hum. Mol. Genetics* **9**, 1779–1786.

Knapp, S., Ladenstein, R., and Galinski, E.A. (1999) *Extremophiles* **3**, 191–198.

Koretz, J. F. and Handelman, G.H. (1988) *Sci. Amer.* **259**, 92–99.

Koteiche, H.A. and Mchaourab, H.S. (1999) *J. Mol. Biol.* **294**, 561–577.

Kretschmar, M. (1999) *Ph.D. Thesis*, University of Regensburg.

Kretschmar, M. and Jaenicke, R. (1999) *J. Mol. Biol.* **291**, 1147–1153.

Kretschmar, M., Mayr, E.-M., and Jaenicke, R. (1999a) *Biol. Chem.* **380**, 89–94.

Kretschmar. M., Mayr, E.-M., and Jaenicke, R. (1999b) *J. Mol. Biol.* **289**, 701–705.

Kröger, R.H.H., Campbell, M.C.W., Munger, R., and Fernald, R.D. (1994) *Vision Res.* **34**, 1815–1822.

Kumar, L.V. and Rao, C.M. (2000) *J. Biol. Chem.* **275**, 22009–22013.

Kumaraswamy, V.S., Lindley, P.F., Slingsby, C., and Glover, I.D. (1996) *Acta Cryst.* **D52**, 611– 622.

Lampi, K.J., Ma, Z., Shih, M., Shearer, T.R., Smith, D.L., and David, L.L. (1997) *J. Biol. Chem.* **272**, 2268–2275.

Lampi, K.J., Ma, Z.X., Hanson, S.R A., Azuma, M., Shih, M., Shearer, T.R., Smith, D.L., Smith, J.B., and David, L.L. (1998) *Exp. Eye Res.* **67**, 31–43.

Lansbury, P.T. (1999) *Proc. Natl. Acad. Sci. USA* **96**, 3342–3344.

Lapatto, R., Nalini, V., Bax, B., Driessen, H., Lindley, P.F., Blundell, T.L., and Slingsby, C. (1991) *J. Mol. Biol.* **222**, 1067–1083.

Lauffer, M.A. (1975) *Entropy-driven Processes in Biology*. Springer Verlag, Berlin.

Ledl, F. and Schleicher, E. (1990) *Angew. Chem. Int. Ed.* **102**, 565–594.

Lee, G.J., Roseman, A.M., Saibil, H.R., and Vierling, E. (1997) *Embo J.* **16**, 659–671.

Lindner, R.A. and Ralston, G.B. (1995) *Biophys. Chem.* **57**, 15–25.

Lindner, R.A. and Ralston, G.B. (1997) *Biophys. Chem.* **66**, 57–66.

Liu, C.W., Asherie, N., Lomakin, A., Pande, J., Ogun, O., and Benedek, G.B. (1996) *Proc. Natl. Acad. Sci. USA* **93**, 377–382.

Lubsen, N.H., Aarts, H.J.M., and Schoenmakers, J.G.G. (1988) *Progr. Biophys. Mol. Biol.* **51**, 47–76.

Ma, Z.X., Hanson, H.R.A., Lampi, K.J., David, L.L., Smith, D.L., and Smith, J.B. (1998) *Exp. Eye. Res.* **67**, 21–30.

MacRae, T.H. (2000) *Cell Mol. Life Sci.* **57**, 899–913.

Makhatadze, G.I. and Privalov, P.L. (1995) *Adv. Protein Chem.* **47**, 307–425.

Maiti, M., Kono, M. and Chakrabarti, B. (1988) *FEBS Letters* **236**, 109–114.

Matthews, B.W. (1993) *Annu. Rev. Biochem.* **62**, 139–160.

Matthews, B.W. (1996) *FASEB J.* **10**, 35–41.

Maxwell, J.C. (1854) *Cambridge and Dublin Mathematical J.* **8**, 188–195.

Mayr, E.-M. (1995) *Ph.D. Thesis,* University of Regensburg.

Mayr, E.-M., Jaenicke, R., and Glockshuber, R. (1994) *J. Mol. Biol.* **235**, 84–88.

Mayr, E.-M., Jaenicke, R., and Glockshuber, R. (1997) *J. Mol. Biol.* **269**, 260–269.

Merck, K.B., Groenen, P.J.T.A., Voorter, C.E.M., de Haard-Hoekman, W.A., Horwitz, J., Bloemendal, H., and de Jong, W.W. (1993) *J. Biol. Chem.* **268**, 1046–1052.

Minton, A. (1998) *Meth. Enzymol.* **295**, 127–149.

Minton, A. (2000a) *Biophys. J.*, **78**, 101–109.

Minton, A. (2000b) *Curr. Opin. Struct. Biol.* **10**, 34–39.

Mok, Y.K., de Prat Gay, G., Butler, P.J., and Bycroft, M. (1996) *Protein Sci.* **5**, 310–319.

Muchowski, P.J., Hays, L.G., Yates, J.R., and Clark, J.I. (1999) *J. Biol. Chem.* **274**, 30190–30195.

Murphy, K.P. (1995) In: *Protein Stability and Folding* (B.A. Shirley, Ed.) Humana Press, Totowa, NJ, 1–34.

Myers, J.K., Pace, C.N., and Scholz, M. (1995) *Protein Sci.,* **4**, 2138–2148.

Nagl, S.B. (2001) In: *Genotype and Phenotype,* 2nd ed. (Malcolm, S. and Goodship, J., Eds.) Bios Scientific Publishers, Oxford, in press.

Najmudin, S., Nalini, V., Driessen, H.P.C., Slingsby, C., Blundell, T.L., Moss, D.S., and Lindley, P.F. (1993) *Acta Crystallogr. Sect. D* **49**, 223–233.

Neet, K.E. and Timm, D.E. (1994) *Protein Sci.* **3**, 2167–2174.

Norledge, B.V., Mayr, E.-M., Glockshuber, R., Bateman, O.A., Slingsby, C., Jaenicke, R. and Driessen, H.P.C. (1996) *Nature Struct. Biol.* **3**, 267–274.

Norledge, B.V., Hay, R.E., Bateman, O.A., Slingsby,C., and Driessen, H.P.C. (1997a) *Exp. Eye Res.* **65**, 609–630.

Norledge, B.V., Trinkl, S., Jaenicke, R., and Slingsby, C. (1997b) *Protein Sci.* **6**, 1612–1620.

Nugent, J. and Whelan, J. (Eds.) (1984) *Human Cataract Formation*. Ciba Found. Symp. **106**.

Ogasahara, K., Nakamura, M., Nakura, S., Tsunasawa, S., Kato, I., Yoshimoto, T., and Yutani, K. (1998) *Biochemistry* **37**, 17537–17544.

Ohno, A., Tate, S.-I., Seeram, S.S., Hiraga, K., Swindells, M.B., Oda, K., and

Kainosho, M. (1998) *J. Mol. Biol.* **282**, 421–433.

Opitz, U., Rudolph, R., Jaenicke, R., Ericsson, L., and Neurath, H. (1987) *Biochemistry* **26**, 1399–1406.

Pace, C.N. (1986) *Meth. Enzymol.* **131**, 266–280.

Pace, C.N. and Scholtz, J.M. (1997) In: *Protein Structure: A Practical Approach* (Creighton, T.E., Ed.) IRL, Oxford, 299–321.

Pace, C.N., Shirley, B.A., McNutt, M., and Gajiwala, K. (1996) *FASEB. J.* **10**, 75–83.

Palme, S., Slingsby, C., and Jaenicke, R. (1997) *Protein Sci.* **6**, 1529–1536.

Palme, S., Jaenicke, R., and Slingsby, C. (1998a) *Protein Sci.* **7**, 611–618.

Palme, S., Jaenicke, R., and Slingsby, C. (1998b) *J. Mol. Biol.* **279**, 1053–1059.

Pan, F-M., Chang, W.-C., Chao, Y.-K., and Chiou, S.H. (1995) *Biochem. Biophys. Res. Commun.* **202**, 527–534.

Pande, J., Lomakin, A., Fine, B. Ogun. O., Sokolinski, I., and Benedek, G.B. (1995) *Proc. Natl. Acad. Sci. USA* **92**, 1076–1071.

Pande, A., Pande, J., Asherie N., Lomakin, A., Ogun, O., King, J.A., Lubsen, N.H., Walton, D., and Benedek, G.B. (2000) *Proc. Natl. Acad. Sci. USA* **97**, 1993–1998.

Pappenberger, G., Schurig, H., and Jaenicke, R. (1997) *J. Mol. Biol.* **274**, 676–683.

Parsegian, V.A., Rand, R.P., Fuller, N.L., and Rau, D.C. (1986) *Meth. Enzymol.* **127**, 400–416.

Perl, D., Welker, C., Schindler, T., Schröder, K., Marahiel, M.A., Jaenicke, R., and Schmid, F.X. (1998) *Nature Struct. Biol.* **5**, 229–235.

Perl, D., F.X., Mueller, U., Heinemann, U., and Schmid, F.X. (2000) *Nature Struct. Biol.* **7**, 380–383.

Perutz, M.F. and Raidt, H. (1975) *Nature* **255**, 256–259.

Pfeil, W. (1981) *Mol. Cell. Biochem.* **40**, 3–28.

Pfeil, W. (1998) *Protein Stability and Folding*. Springer Verlag, Berlin, Heidelberg, New York.

Piatigorsky, J. and Wistow, G.J. (1989) *Cell* **57**, 197–199.

Piatigorsky, J. and Wistow, G. (1991) *Science* **252**, 1078–1079.

Piatigorsky, J. and Zelenka, P.S. (1992) *Adv. Dev. Biochem.* **1**, 211–256

Pierscionek, B.K. (1997) *Exp. Eye Res.* **64**, 887–893.

Pierscionek, B.K. and Augusteyn, R.C. (1992) *Biochim. Biophys. Acta* **1116**, 283–290.

Plaxco, K.W. and Baker, D. (1998) *Proc. Natl. Acad. Sci. USA* **95**, 13591–13596.

Podos, S.M. and Yanoff, M. (Eds.) (1992) *Textbook of Ophthalmology*. Gower Medical Publishing, New York, London.

Privalov, P.L. (1979) *Adv. Protein Chem.* **33**, 167–241.

Privalov, P.L. (1982) *Adv. Protein Chem.* **35**, 193–231.

Privalov, P.L. (1992) In: *Protein Folding* (T.E. Creighton, Ed.) Freeman, New York, 83–126.

Privalov, P.L. and Gill, S.J. (1988) *Adv. Protein Chem.* **39**, 193–231.

Raman, B., Ramakrishna, T. and Rao, C.M. (1995) *J. Biol. Chem.* **270**, 19888–19892.

Ray, M.E., Wistow, G.J., Su, Y.A., Meltzer, P.S., and Trent, J.M. (1997) *Proc. Natl. Acad. Sci. U.S.A.* **94**, 3220–3234.

Reddy, G.B., Das, K.P., Petrash, J.M., and Surewicz, W.K. (2000) *J. Biol. Chem.* **275**, 4565–4570.

Rivas, G., Fernandez, J.A., and Minton, A.P. (1999) *Biochemistry* **38**, 9379–9388.

Rosinke, B., Renner, C., Mayr, E.-M., Jaenicke, R., and Holak, T.A. (1997) *J. Mol. Biol.* 645–655.

Rudolph, R., Siebendritt, R., Nesslauer, G., Sharma, A.K., and Jaenicke, R. (1990) *Proc. Natl. Acad. Sci. USA* **87**, 4625–4629.

Saibil, H. (2000) *Curr. Opin. Struct. Biol.* **10**, 251–258.

Sauer, H.W. (1986) In: *The Molecular Biology of Physarum polycephalum*. (Dove, W.F., Dee, J., Hatano, S., Haugli, F.B. and Wohlfarth-Bottermann, K.E., Eds.). Plenum Press, New York, 1–17.

Schellman, J.A. (1997) *Biophys. J.* **73**, 2960–2964.

Schindler, T., Herrler, M., Marahiel, M.A., and Schmid, F.X. (1995) *Nature Struct. Biol.* **2**, 663–673.

Schlunegger, M.P., Bennett, M.J., and Eisenberg, D. (1997) *Adv. Protein Chem.* **50**, 61–122.

Sharma, A.K., Minke-Gogl, V., Gohl, P., Siebendritt, R, Jaenicke, R., and Rudolph, R. (1990) *Eur. J. Biochem.* **194**, 603–609.

Shirley, B.A., Stanssens, P., Hahn, U., and Pace, C.N. (1992) *Biochemistry* **31**, 725–732.

Siezen, R.J., Fisch, M.R., Slingsby, C., and Benedek, G.B. (1985) *Proc. Natl. Acad. Sci. USA* **82**, 1701–1705.

Siezen, R.J., Wu, E., Kaplan, E.D., Thomson, J.A., and Benedek, G.B. (1988) *J. Mol. Biol.* **199**, 475–490.

Slingsby, C. (1985) *Trends. Biochem. Sci.* **10**, 281–284.

Slingsby, C. and Bateman, O.A. (1990) *Biochemistry* **29**, 6592–6599.

Slingsby, C. and Clout, N.J. (1999) *Eye* **13**, 395–402.

Slingsby, C. and Croft, L.R. (1978) *Exp. Eye Res.* **26**, 291–304.

Slingsby, C., Bax, B., Lapatto, R., Bateman, O.A., Driessen, H., Lindley, P.F, Moss, D.S., Najmudin, S., and Blundell, T. (1991). In: *Presbyopia Research: From Molecular Biology to Visual Adaptation* (Obrecht, G. and Stark, L.W., Eds.). Plenum Press, New York, 41–48.

Slingsby, C., Norledge, B., Simpson, A., Bateman, O.A., Wright, G., Driessen, H.P.C., Lindley, P.F., Moss, D.S., and Bax, B. (1997) *Progr. Ret. Eye Res.* **16**, 3–29.

Smith, G., Atchison, D.A., and Pierscionek, B.K. (1992. *J. Opt. Soc. Am. A* **9**, 2111–2117.

Spector, A., Freund, T., Li, L.K., and Augusteyn, R.C. (1971) *Invest. Ophthalmol.* **10**, 677–686.

Surewicz, W.K. and Oleson, P.R. (1995) *Biochemistry* **34**, 9655–9660.

Suzuki, Y. (1989) *Proc. Japan Acad. Ser. B, Phys. Biol. Sci.* **65**, 146–148.

Suzuki, Y. (1992) In: *Industrial Biotechnology* (Malik, V.S. and Sridhar, P., Eds.). Oxford and IBH Publ. Co., New Delhi, 163–178

Takemoto, L. and Boyle, D. (2000) *Molecular Vision* **6**, 164–168.

Tamura A. and Privalov, P.L. (1997) *J. Mol. Biol.* **273**, 1048–1060

Tanaka, T. and Benedek, G. (1975) *Invest. Ophthalmol.* **14**, 449–456.

Tanford, C. (1968) *Adv. Protein Chem.* **23**, 121–282.

Tanford, C. (1970) *Adv. Protein Chem.* **24**, 1–95.

Tanford, C. (1973) *The Hydrophobic Effect*. John Wiley, New York.

Tardieu, A. and Delaye, M. (1988) *Annu. Rev. Biophys. Chem.* **17**, 47–70.

Tardieu, A. and Vérétout, F. (1991) In: *Presbyopia Research: From Molecular Biology to Visual Adaptation* (Obrecht, G. and Stark, L.W., Eds.). Plenum Press, New York, 49–55.

Tardieu, A., Vérétout, F., Krop, B., and Slingsby, C, (1992) *Eur. Biophys. J.* **21**, 1–12.

Tardieu, A., Le Verge, A., Malfois, M., Bonneté, F., Finet, S., Riés-Kautt, M., and Belloni, L. (1999) *J. Crystal Growth* **196**, 193–203.

Teintze, M., Inouye, M., and Inouye, S. (1988) *J. Biol. Chem.* **263**, 1199–1203.

Teintze, M., Inouye, M., and Inouye, S. (1991) In: *Novel Calcium-binding Proteins*. (Heizmann, C.W., Ed.) Springer Verlag, New York, 437–446.

Tellam, R.L., Sculley, M.J., Nicol, L.W., and Wills, P.R. (1983) *Biochem. J.* **213**, 651–659.

Thirumalai, D. and Lorimer, G. (2001) *Annu. Rev. Biophys. Biomol. Struct.*, **30**, 245–269.

Thompson, K.S., Vinson, C.R., and Freire, E. (1993) *Biochemistry* **32**, 5491–5496.

Thompson, M.J. and Eisenberg, D. (1999) *J. Mol. Biol.* **290**, 595–604.

Thornton, J.M. (2001) *Protein Sci.* **10**, 3–11.

Timasheff, S.N. (1992) In: *Water and Life* (Somero, G.N., Ed.) Springer, New York, 70–84.

Timasheff, S.N. and Arakawa, T. (1997) In: *Protein Structure: A Practical Approach* (Creighton, T.E., Ed.) IRL, Oxford, 349–364.

Tomschy, A., Böhm, G., and Jaenicke, R. (1994) *Protein Eng.* **7**, 1471–1478.

Treweek, T.M., Lindner, R.A., Mariani, M., and Carver, J.A. (2000) *Biochim. Biophys. Acta Prot. Struc. Mol. Enz.* **1481**, 175–188.

Trinkl, S., Glockshuber, R., and Jaenicke, R. (1994) *Protein Sci.* **3**, 1392–1400.

Truscott, R.J.W. (2000) *Ophthalmic Res.* **32**, 185–194.

van Boekel, M.A.M., van Aalten, D.M., Caspers, G.-J., Röll, B., and de Jong, W.W. (2001) *J. Mol. Evol.*, **52**, 239–248.

van den Berg, , B., Ellis, R.J., and Dobson, C.M. (1999) *EMBO J.* **18**, 6927–6933.

van den Berg, B., Wain, R., Dobson, C.M., and Ellis, R.J. (2000) *EMBO J.* **19**, 3870–3875.

van den Oetelaar, P.J. and Hoenders, H.J. (1989) *Biochem. Biophys. Acta* **995**, 91–96.

van Holde, K.E., Johnson, W.C., and Ho, P.S. (1998) *Principles of Physical Biochemistry*. Prentice Hall Int., Upper Sddle River, NJ.

Vanhoudt, J., Abgar, S., Aerts, T., and Clauwaert, J. (2000) *Biochemistry* **39**, 4483–4492.

van Oss, C.J. (1993) In: *Water and Biological Macromolecules* (Westhof, E., Ed.). Macmillan Press, Houndmills and London, 393–429.

van Oss, C.J. and Good, R.J. (1988) *J. Protein Chem.* **7**, 179–183.

Vérétout, F., Delaye, M., and Tardieu, A. (1989) *J. Mol. Biol.* **205**, 713–728.

Volkin, D.B., Mach, H., and Middaugh, C.R. (1995) In: *Protein Stability and Folding* (Shirley, B.A., Ed.). *Meth. Mol. Biol.* Vol. 40, 35–63.

Wang, K. and Spector, A. (2000) *Eur. J. Biochem.* **267**, 4705–4712.

Welch, W.J., Eggers, D.K., Hansen, W.J., and Nagata, H. (1998) In: *Molecular Chaperones in the Life Cycle of Proteins* (Fink, A.L. and Goto, Y., Eds.) Marcel Dekker, New York, 71–93.

Wenk, M. (1999) *Ph.D. Thesis,* University of Regensburg.

Wenk, M. and Mayr, E.-M. (1998) *Eur. J. Biochem.* **255**, 604–610.

Wenk, M. and Jaenicke, R. (1999) *J. Mol. Biol.* **293**, 117–124.

Wenk, M., Jaenicke, R., and Mayr, E.-M. (1998) *FEBS Lett*. **438**, 127–130.

Wenk, M., Baumgartner, R., Holak, T.A., Huber, R., Jaenicke, R., and Mayr, E.-M. (1999) *J. Mol. Biol.* **286**, 1533–1545.

Wenk, M., Herbst, R., Hoeger, D., Kretschmar, M., Lubsen, N.H., and Jaenicke, R. (2000) *Biophys. Chem.* **86**, 95–108.

Werten, P.J.L., Vos, E., and de Jong W.W. (1999) *Exp. Eye Res*. **68**, 99–103.

Werten, P.J.L. Carver, J.A., Jaenicke, R., and de Jong W.W. (1996) *Prot. Eng*. **9**, 1021–1028.

Werten, P.J.L., Lindner, R.A., Carver, J.A., and de Jong, W.W. (1999) *Biochim. Biophys. Acta* **1432**, 286–292.

Werten, P.J.L., Röll, B., van Aalten, D.M.F., and de Jong. W.W. (2000) *Proc. Natl. Acad. Sci. U.S.A.* **97**, 3282–3287.

Wetlaufer, D.B. (1980) In: *Protein Folding* (Jaenicke, R., Ed.). Elsevier/North-Holland, Amsterdam, New York, 323–329.

Wickner, S., Maurizi, M.R., and Gottesman, S. (1999) *Science* **286**, 1888–1893.

Wieligmann, K. (1996) *Diploma Thesis*, University of Regensburg.

Wieligmann, K. (2000) *Ph.D. Thesis*, University of Regensburg.

Wieligmann, K., Norledge, B.V., Jaenicke, R., and Mayr, E.-M. (1998) *J. Mol. Biol*. **280**, 721–729.

Wieligmann, K., Mayr, E.-M., and Jaenicke, R. (1999) *J. Mol. Biol*. **286**, 989–994.

Wilf, J., Gladner, J.A., and Minton, A.P. (1985) *Thromb. Res.* **37**, 681–688.

Wireman, J.W. and Dworkin, M. (1977) *J. Bacteriol*. **129**, 796–802.

Wistow, G. (1990) *J. Mol. Evol*. **30**, 140–145.

Wistow, G. (1993) *Trend. Biochem. Sci*. **18**, 301–306.

Wistow, G. (1995) In: *Molecular Biology and Evolution of Crystallins*. Mol. Biol. Springer Verlag, Landes, Austin, TX, 37–82.

Wistow, G. and Piatigorsky, J. (1987) *Science* **236**, 1554–1556.

Wistow, G.J. and Piatigorsky, J. (1988) *Annu. Rev. Biochem*. **57**, 479–504.

Wistow, G., Summers, L., and Blundell, T.L. (1985) *Nature* **315**, 771–773.

Wistow, G.J., Mulders, J.W., and de Jong, W.W. (1987) *Nature* **326**, 622–624.

Wistow, G., Anderson, A., and Piatigorsky, J. (1990) *Proc. Natl. Acad. Sci. U.S.A.* **87**, 6277–6280.

Wright, G., Basak, A.K., Wieligmann, K., Mayr, E.-M., and Slingsby, C. (1998) *Protein Sci.* **7**, 1280–1285.

Yamamoto, T., Hiratani, T., Hirata, H., Imai, M., and Yamaguchi, H. (1986) *FEBS Lett.* **197**, 50–54.

Yip, K.S.P., Britton, K.L., Stillman, K.L., Lebbink, J., de Vos, W.M., Robb, F.T., Vetriani, C., Maeder, D., and Rice, D.W. (1998) *Eur. J. Biochem.* **255**, 336–346.

Zarina, S., Slingsby, C., Jaenicke, R., Zaidi, Z.H., Driessen, H., and Srinivasan, N. (1994) *Protein Sci.* **3**, 1840–1846.

Zimmerman, S.B. and Minton, A.P. (1993) *Annu. Rev. Biophys. Biomol. Struct.* **22**, 27–65.